Atmos. Chem. Phys. Discuss., doi:10.5194/acp-2016-1037, 2016
Manuscript under review for journal Atmos. Chem. Phys.
Published: 14 December 2016

Atmospheric Chemistry and Physics Discussions

Arctic aerosol net indirect effects on thin, mid-altitude, liquid-bearing clouds

Lauren M. Zamora[1,2*], Ralph A. Kahn[2], Sabine Eckhardt[3], Allison McComiskey[4], Patricia Sawamura[5,6], Richard Moore[5], Andreas Stohl[3]

[1]NASA Postdoctoral Program Fellow, Universities Space Research Association
[2]NASA Goddard Space Flight Center, Greenbelt, MD, USA
[3]NILU - Norwegian Institute for Air Research, Kjeller, Norway
[4]NOAA Earth System Research Laboratory, Boulder, CO, USA
[5]NASA Langley Research Center, Hampton, VA, USA
[6]Science Systems and Applications, Inc., Greenbelt, MD, USA

Correspondence to: Lauren M. Zamora (lauren.m.zamora@nasa.gov)

Abstract. Aerosol indirect effects have uncertain, but potentially large, impacts on the Arctic energy budget. Here, we have reduced uncertainty in current-day Arctic net aerosol indirect effects on the surface by better constraining various physical and microphysical characteristics of optically thin, liquid-containing clouds in clean, average and aerosol-impacted conditions using a combination of CALIPSO and CloudSat data and model output. This work provides a foundation for how future observational studies can evaluate previous model estimates of the aerosol indirect effect. Clouds over sea ice and open ocean show large differences in surface and meteorological forcing, including a near doubling of multi-layer cloud presence over the open ocean compared to sea ice. The optically thin cloud subset is susceptible to aerosols, and over sea ice we estimate a regional scale maximum net indirect effect on these clouds during polar night equivalent to ~0.6-0.8 W m^{-2} at the surface. Aerosol presence is related to reduced precipitation, cloud thickness, and radar reflectivity, and may be associated with an increased likelihood of cloud presence in the liquid phase. The observations are consistent with a thermodynamic indirect effect hypothesis and are inconsistent with a glaciation indirect effect.

1 Introduction

Aerosol indirect effects on clouds are among the biggest uncertainties in climate models (Boucher et al., 2013). It is particularly important to reduce these uncertainties in the Arctic, where warming is occurring at a faster rate than in other locations (Serreze et al., 2009), and where local aerosol indirect effects can be large (Garrett et al., 2004; Garrett and Zhao, 2006; Lubin and Vogelmann, 2006; Zhao and Garrett, 2015). In addition, understanding aerosol indirect effects is important

Atmos. Chem. Phys. Discuss., doi:10.5194/acp-2016-1037, 2016
Manuscript under review for journal Atmos. Chem. Phys.
Published: 14 December 2016

because aerosol emissions within and in the vicinity of the Arctic are changing, and perhaps more importantly, the major aerosol removal processes and transport pathways to the Arctic may be changing as well (Jiao and Flanner, 2016).

Unfortunately, accurate observation-based estimates of regional mean forcings are very difficult to obtain at most locations around the planet due to a variety of confounding factors and errors. These include: 1) a reliance on proxies for cloud condensation nuclei (CCN) and ice nucleating particles (INP), 2) meteorological co-variability and other synoptic-scale surface and atmospheric factors, including the aerosol spatial distribution, 3) the complexity of cloud responses to aerosol type and amount, 4) spatial and temporal limitations of the datasets, and 5) an insufficient understanding of cloud characteristics even in the absence of anthropogenic aerosols (Ghan et al., 2016; Wilcox et al., 2015). Knowledge of this last factor is difficult to obtain because pristine conditions are rare in most locations globally (Hamilton et al., 2014). To quantify mean regional aerosol indirect effects using observations, one would need datasets that cover the large spatial and temporal scales needed to include the full range of natural heterogeneity, plus a way to correctly identify clean background conditions. As a result, current estimates of net regional indirect aerosol impacts on the surface radiation rely predominantly upon models that still cannot accurately represent many relevant Arctic processes (e.g., Morrison et al. (2012); Ovchinnikov et al. (2014)).

In some ways, isolating aerosol indirect effects in the Arctic can be even more challenging than in other regions. Sampling conditions at the ground are harsh, there is low thermal and visible contrast between the surface and clouds, and observations are limited by the frequent presence of multi-layer clouds. The very cold temperatures that characterize the Arctic affect chemical reactions and physical processes (e.g., the development of frost flowers, diamond dust, and blowing snow), making comparisons with lower latitude systems more challenging. However, the Arctic is ideal for the study of net indirect effects in other ways. For example, pristine conditions still occur in this region with relatively high frequency, despite periodic episodes of transport of combustion-derived aerosols from lower latitudes. Moreover, the surface and meteorological conditions over sea ice are highly homogenous compared to many other regions of the world.

Here we present a method for identifying spatially distributed properties of clean, optically thin (i.e., cloud optical depth, COD < 3) liquid Arctic background clouds using a combination of active remote sensing instruments, CALIPSO and CloudSat, and an atmospheric transport model. We use the difference between average cloud characteristics gathered across the Arctic and average clean background clouds over the same region to estimate the maximum net indirect aerosol impacts on the surface. This calculation provides an estimate of the actual regional impact of aerosol indirect effects on the surface including aerosol-meteorological co-variability after stochastic meteorological effects have been taken into account. We also examine differences between the cloud characteristics under various aerosol conditions to assess cloud formation mechanisms in the presence of aerosol.

Atmos. Chem. Phys. Discuss., doi:10.5194/acp-2016-1037, 2016
Manuscript under review for journal Atmos. Chem. Phys.
Published: 14 December 2016

Atmospheric Chemistry and Physics Discussions

In this study, we focus on mid-level, optically thin, predominantly liquid clouds during polar night. These clouds are easy for CALIPSO to observe, and this enables us to identify clean background conditions with a high degree of precision. These optically thin, liquid-containing clouds are very common in the Arctic (Bennartz et al., 2013; Shupe and Intrieri, 2004). They also are effective at radiating longwave (LW) radiation downward (e.g., Garrett and Zhao (2006)) and they make a strong contribution to surface forcing (Shupe and Intrieri, 2004). Moreover, due to reduced liquid water content, the emissivity of this type of cloud is more susceptible than thicker clouds to aerosol influences. Models tend to under-predict the formation of these optically thin clouds at supercooled temperatures (Cesana et al., 2012), making aerosol influences on droplet characteristics and ice nucleation of particular interest.

2 Methods

2.1 Sample selection

To describe aerosol impacts on Arctic clouds with high confidence using CALIPSO and CloudSat data, we selected a specific group of clouds where non-background aerosol (hereafter referred to simply as "aerosol") conditions and cloud properties could be ascertained with the greatest confidence. This Arctic cloud subset consists of clouds that are Measured > One km above the surface, are Optically thin (COD < ~3), collected at Nighttime, predominantly Liquid, and from the Top-layer, henceforth referred to as "MOONLiT" clouds for brevity. Because the MOONLiT cloud profiles were taken only at night, the majority of them were collected during the winter when there are relatively high aerosol inputs from lower latitudes (Shaw, 1995). Within the full MOONLiT cloud group, we also identified the subsets of MOONLiT clouds present in clean background and aerosol-influenced conditions. The criteria for these classifications, as well as for clear air (no cloud) cases, are summarized in Table 1. Descriptions of these criteria and the individual datasets used for sample selection are described in more detail below.

2.1.1 CALIPSO

Aerosol vertical distribution, cloud top height, cloud base height, cloud optical depth, and initial approximate cloud phase were obtained from the polar-orbiting CALIPSO satellite lidar v. 3.01 level 2, 5-km aerosol profile and cloud layer products at 532 nm. These data have a vertical resolution of 30 m within the vertical region of interest (1-8 km). Before averaging, along-track cloud profile data were collected at a horizontal resolution of 1/3 km. Averaged aerosol data have a horizontal resolution of between 5-80 km, with the horizontal resolution decreasing with aerosol concentration. For example, in clear air with no detected aerosols, the horizontal resolution is 80 km; in strong aerosol layers, the horizontal resolution providing adequate signal-to-noise can be as low as 5 km (Vaughan et al., 2009).

Because our samples were taken at night, Moderate Resolution Imaging Spectroradiometer (MODIS) optical depths were not available. Instead, the CALIPSO product was used to measure CODs, as it offers substantially higher data availability in the

Atmos. Chem. Phys. Discuss., doi:10.5194/acp-2016-1037, 2016
Manuscript under review for journal Atmos. Chem. Phys.
Published: 14 December 2016

Atmospheric Chemistry and Physics Discussions

optical thickness range of interest ($\tau < 3$) than CloudSat (Christensen et al., 2013). Only non-quality-flagged (i.e., the highest quality) CALIPSO COD data were used. CALIPSO cloud optical depth uncertainties rise with COD due to uncertainties in the lidar ratio in liquid clouds with $\tau > 1$ (CALIPSO Quality Statements: Lidar Level 2 Cloud and Aerosol Layer Products, Version releases: 3.01, 3.02). We excluded COD data with uncertainties ≥ 75% of the COD value (these constituted ~8% of all cases).

Because it can be difficult to accurately separate Arctic aerosol from diamond dust and thin ice clouds using backscatter data (*M. Vaughan*, pers. comm.; Grenier and Blanchet (2010)), we focused on CALIPSO liquid-containing clouds, and ice clouds were not allowed in the profile. Note that CALIOP cloud "phase" indicates only whether the cloud predominantly contained liquid or ice; there is no mixed-phase designation. At a later step, CloudSat data were used to further refine cloud phase information.

CALIPSO data were obtained between 60-82°N and between 1 January 2008 – 7 December 2009 (during the latter part of CloudSat epoch 2). To obtain the lowest possible comparable detection limit, the analysis was restricted to upper-layer nighttime clouds. Here, nighttime profiles are taken in the CALIPSO orbit over the hemisphere of Earth that is dark at any given time, and so the borders of this hemisphere may include some low-light conditions. We focused on clouds present between 1 and 8 km above the surface to enable better below-cloud aerosol detection and better comparison to high-quality CloudSat data. In order to detect cloud base height and any strong aerosol layers below-cloud, the analysis was limited to non-opaque clouds ($\tau < \sim 3$), as determined by the 532 nm Extinction Quality Control flag. Clouds were included only when the feature's optical properties scored > 70 out of 100 in the cloud-aerosol discrimination (CAD) algorithm (a high confidence cloud determination)(Liu et al., 2009).

The "clean, background" cloud subset met the above criteria, but no aerosol features were permitted above or below cloud, so that horizontal averaging was high and standard across cases at an 80-km resolution. Given these constraints, the backscatter aerosol detection limit for "clean background" clouds is as low as possible, and should have only negligible variations based on detector noise and background molecular and O_3 densities above cloud (Vaughan et al., 2009). Because CALIPSO cannot always detect dilute aerosols (Di Pierro et al., 2013; Kacenelenbogen et al., 2014; Rogers et al., 2014; Winker et al., 2013), particularly below-cloud where the lidar signal has been reduced, "clean background" clouds were also required to have modeled above and below-cloud FLEXPART ("FLEXible TRAjectory model", (Stohl et al., 1998, 2005)) black carbon concentrations of < 30 ng C m^{-3} (see Sect. 2.1.3 and 3.1 for further discussion). The "aerosol-influenced" subset had aerosols with CAD scores between -100 and -70 (high confidence aerosol classification) above or below the cloud and FLEXPART modeled below-cloud black carbon concentrations of > 30 ng C m^{-3}. The geographical distributions of the all-cloud, clean-cloud, and aerosol-influenced cloud sets are shown in Fig. 1.

Atmos. Chem. Phys. Discuss., doi:10.5194/acp-2016-1037, 2016
Manuscript under review for journal Atmos. Chem. Phys.
Published: 14 December 2016

Atmospheric Chemistry and Physics Discussions

2.1.2 CloudSat

CloudSat cloud profiling radar data are collected at a vertical resolution of 240 m. CloudSat has a wider swath than CALIPSO (1.4x1.8 km) and it takes measurements on the same polar orbit, only seconds ahead of CALIPSO. To ensure comparability of clouds measured with both instruments, only clouds for which the reported cloud top height was within 0.4 km in both instruments were included (i.e., ~95% of the data). Because the CloudSat radar does not accurately estimate cloud properties below ~0.7-1 km agl (Huang et al., 2012; Mioche et al., 2015), we focused on clouds with bases ≥ 1 km agl. We recognize that many Arctic clouds lie below this altitude (Devasthale et al., 2011a; Shupe et al., 2011) and that these low-level clouds have important radiative impacts. However, we still chose to focus on clouds at these higher levels to obtain higher certainty in the data.

Average reflectivity between the CALIPSO-determined cloud top and base was obtained from the CloudSat 2B-GEOPROF version R04 dataset. Cloud phase and precipitation occurrence were acquired from 2B-CLDCLASS-LIDAR version R04 estimates (Wang, 2013). In this product, cloud phase is determined from a combination of CALIPSO water layer detection and integrated backscattering coefficient, temperature, CloudSat reflectivity, and an assumed temperature-dependent reflectivity threshold for ice particles (Zhang et al., 2010). This phase classification is uncertain for clouds with reflectivities of < -29 dBZ (the CloudSat sensitivity limit), and for very thin clouds due to the coarse vertical resolution of the instrument. As we focused on cold, optically thin clouds in this study, many (~25%) of our samples were below the CloudSat detection limit. Thus, phase was only assessed in clouds with cloud phase certainty values of > 5 and with reflectivity values of > -29 dBZ. Infrequently, clouds that met the CALIPSO criterion in Table 1 were classified as predominantly ice phase by the 2B-CLDCLASS-LIDAR product; these cases were excluded from the analysis for simplicity, despite the potential for supercooled water to be misclassified as ice particles (Van Tricht et al., 2016).

Estimated mean liquid cloud droplet effective radii (r_{el}) were obtained from the CloudSat 2B-CWC-RO version R04 product (LO_RO_effective_radius) (Austin and Stephens, 2001). We chose this CloudSat r_{el} product, which assumes that all particles are liquid, for two reasons: 1) CALIPSO had independently assigned the clouds a predominantly liquid phase, and 2) uncertainties in the other liquid r_{el} data product available for nighttime samples (RO_liq_effective_radius) may be fairly high because of a reliance on an overly-simplistic, temperature-dependent phase partitioning scheme (e.g., de Boer et al. (2008); Lee et al. (2010)). Where available, r_{el} data were averaged over vertical regions within the CALIOP-determined "liquid" phase cloud base and top. Sometimes the corresponding CloudSat-determined cloud base and top were slightly different. In these cases, CALIOP heights were used because of its better ability to detect liquid droplets, and because CloudSat may sometimes misclassify precipitating ice as part of the cloud (de Boer et al., 2008), which can lead to overestimation of r_{el}. Quality-flagged data were excluded, such as observations from precipitating clouds, as determined from the CloudSat 2B-CLDCLASS-LIDAR version R04 product. Note: although we counted the number of cases where precipitation occurred for comparison at a different step, precipitating cases were otherwise excluded from the analysis.

Atmos. Chem. Phys. Discuss., doi:10.5194/acp-2016-1037, 2016
Manuscript under review for journal Atmos. Chem. Phys.
Published: 14 December 2016

Atmospheric Chemistry and Physics Discussions

We present some limited CloudSat-derived r_{el} data here, but it is important to note the fairly high uncertainties in some of these data. Aside from the assumption of liquid phase, there is a known bug in the CloudSat code that might cause r_{el} in liquid clouds to be overestimated, and to our knowledge there has been no extensive validation of the CloudSat 2B-CWC-RO r_{el} product in the Arctic. de Boer et al. (2008) found fairly reasonable agreement, with perhaps some overestimation, between CloudSat-determined r_{el} in mixed-phase clouds compared to r_{el} measured from ground-based instruments. However, only a few samples were collected with the in-cloud constraint in that study. The cumulative uncertainties in r_{el} on the radiative impact results are discussed and dealt with further in Sect. 3.5.

2.1.3 FLEXPART

The locations of combustion aerosol plumes were modeled using BC from the FLEXPART model (Stohl et al., 1998, 2005). The FLEXPART model has been used extensively to study pollution and smoke transport in the Arctic, and is well-validated for this purpose (Damoah et al., 2004; Eckhardt et al., 2015; Forster et al., 2001; Paris et al., 2009; Sodemann et al., 2011; Stohl et al., 2002, 2003, 2015). We chose BC as a combustion aerosol tracer because it represents aerosol removal better than a gaseous tracer like carbon monoxide, and because FLEXPART can largely capture the Arctic BC seasonal cycle (Eckhardt et al., 2015) that is driven by a combination of seasonal changes in emissions, atmospheric transport patterns and removal processes. In some cases, wildfires can emit large amounts of light absorbing organic carbon aerosols (or "brown carbon") without emitting large amounts of BC (e.g., Chakrabarty et al. (2016)). In these cases, FLEXPART BC may not represent smoke aerosols well.

For this study, as in Eckhardt et al. (2015), FLEXPART was driven with meteorological analysis data from the European Centre for Medium-Range Weather Forecasts (ECMWF) at a resolution of 1˚ longitude and 1˚ latitude. BC emissions were based on the ECLIPSE emission inventory (Stohl et al., 2015), which also includes emissions from gas flaring, and biomass burning emissions. In the model simulations, BC was removed from the atmosphere through dry deposition, and wet scavenging both below and within clouds. However, no transformation of BC from a hydrophobic to a hydrophilic state was considered and removal parameters were chosen as typical for a hydrophilic aerosol. FLEXPART-modeled BC concentrations were calculated for the years 2008 and 2009 at a horizontal resolution of 1^o latitude and 2^o longitude and at 0.05, 0.2, 1, 2, 3, 5, 7, and 10 km agl. Below-cloud BC concentrations were taken to be the closest modeled concentration available to 0.5 km below cloud base. When there were multi-layer clouds and the next cloud top was < 1 km away, the concentration closest to the middle distance between the two clouds was used instead.

2.2 Ancillary datasets

Aircraft out-of-cloud black carbon data were obtained from NASA's Arctic Research of the Composition of the Troposphere from Aircraft and Satellites (ARCTAS) campaign (Fuelberg et al., 2010; Jacob et al., 2010; Kondo et al., 2011). Submicron aerosol dry size distributions between 0.06–1 μm were measured from a DMT Ultra-High Sensitivity Aerosol Spectrometer

Atmos. Chem. Phys. Discuss., doi:10.5194/acp-2016-1037, 2016
Manuscript under review for journal Atmos. Chem. Phys.
Published: 14 December 2016

Atmospheric Chemistry and Physics Discussions

(UHSAS) between 0-2.1 km (2.9 km for springtime samples). Submicron aerosol scattering data at 532 nm were obtained from a Radiance Research (RR) nephelometer and were corrected for truncation errors. Submicron aerosol scattering coefficients at 450 and 700 nm were estimated as the difference between total scattering from a TSI 3563 Integrating Nephelometer and the RR nephelometer when the fine mode aerosol fraction exceeded 0.6. Ambient total scattering coefficients at the three wavelengths were obtained from the TSI nephelometer, and were corrected for truncation errors following Anderson and Ogren (1998). Aerosol absorption coefficients at 450, 532, and 700 nm were measured with a RR three-wavelength Particle Soot Absorption Photometer (PSAP). Aerosol data were limited to out-of-cloud samples, as determined by measured liquid and ice water contents of zero. For better comparison to the data used in the rest of this study, aircraft data were limited to samples taken between 50-82^{o} N (subarctic + Arctic).

An aircraft-derived, 180^{o} backscatter coefficient is calculated following Sawamura et al., in prep. in order to compare the in situ data to that from CALIOP (units of Mm^{-1} sr^{-1}). First, the measured dry, submicron aerosol size distribution, scattering coefficient, and absorption coefficient at 532 nm are input into a Mie theory model to determine the aerosol effective dry refractive index. Next, a hygroscopic growth factor was applied to the dry size distribution in the Mie theory model to reproduce observed humidified light scattering and thus derive the aerosol refractive index at ambient relative humidity. The 180^{o} backscatter coefficient then follows from Mie theory using the adjusted size distribution and refractive index. This method is best suited for spherical particles, which we assume dominate the ARCTAS samples based on the main aerosol sources during the campaign (non-dust background aerosols, anthropogenic pollution and smoke (Jacob et al., 2010)).

Several other supplemental datasets were used for cloud environmental context. ETOPO1 Bedrock GMT4 data (Amante and Eakins, 2009) were used to determine whether a cloud profile was sampled over a terrestrial or ocean region. NOAA/NSIDC Climate Data Record of Passive Microwave Sea Ice Concentration, version 2 data (Meier et al., 2013; Peng et al., 2013) were used to approximate the fractional sea ice cover over ocean at the specific month and location of each profile. A sample was classified as being primarily over sea ice or open ocean when the sea ice fraction at the given location and month was > 80% or < 20%, respectively.

Lastly, integrated surface longwave (4 -30 μm) radiation was calculated with an updated Santa Barbara DISTORT Atmospheric Radiative Transfer program (SBDART, (Ricchiazzi et al., 1998)). Shortwave effects are not expected to be significant during nighttime conditions. Following McComiskey and Feingold (2008), the calculations assume homogeneous cloud cover and spectrally uniform surface albedo (the implications of which are discussed later). Median surface longwave reflectivity (R) for open ocean and sea ice in clear conditions with no clouds or aerosols (0.64 and 0.69, respectively) was calculated from MERRA 2 output (GMAO, 2015) based on the times and locations of the data and the following formula (Josey, 2003):

Atmos. Chem. Phys. Discuss., doi:10.5194/acp-2016-1037, 2016
Manuscript under review for journal Atmos. Chem. Phys.
Published: 14 December 2016

Atmospheric Chemistry and Physics Discussions

$$R = 1 - \frac{E - A}{I}, \quad (1)$$

where E is the emitted longwave radiation from the surface, A is the net longwave flux across the ocean-atmosphere interface (assuming transmission is negligible),and I is the downwelling longwave radiation from the atmosphere.

2.3 Notes on potential sources of bias and uncertainty imposed by the methods

We imposed artificial criteria to select cloud profiles with the least amount of uncertainty in our parameters of interest. In doing so, we may be inducing some uncertainties in our analysis. For example, due to the low COD constraint, it is possible that some fraction of the cloud subset influenced by aerosols may be selected from a different group of cloud types than some fraction of the clean background cloud subset. As an illustration, in a subarctic aircraft case study presented in Zamora et al. (2016) (see Appendix A for further details), cumulus clean background clouds with an observed cloud thickness of ~250 m had CODs of ~5. These clouds would have been too optically thick for the CALIOP lidar to penetrate. However, highly comparable nearby clouds in a smoke plume had CODs of only ~2, and the cloud-property differences were likely driven by the aerosol (Zamora et al., 2016). In this example, only the subset of clouds influenced by smoke aerosols would have met this study's COD criterion and not the clean background cloud counterparts. Median reductions in COD were fairly minor for aerosol-impacted clouds relative to background clouds, and were not significant over open ocean, and so we do not expect this effect to have a large impact on our study.

Similarly, any aerosol-driven phase changes that shifted clouds between predominantly ice- and liquid-containing clouds (e.g., Girard et al. (2013)) could have eliminated or added samples from/to our study, also potentially adding some bias to our results. These uncertainties are difficult to quantify.

3 Results and Discussion

3.1 Correct identification of clean background conditions

To accurately characterize clean background conditions, it is necessary to detect combustion-related aerosol layers with confidence. For CALIPSO, dilute aerosols are least likely to be detected below-cloud due to signal attenuation inside the cloud (Di Pierro et al., 2013), but CALIOP can sometimes miss dilute aerosol layers even in clear air above clouds (Di Pierro et al., 2013; Kacenelenbogen et al., 2014; Rogers et al., 2014; Sheridan et al., 2012; Winker et al., 2013). Most previous works focused either on daytime samples, which have comparatively low signal-to-noise ratios, or on extinction data, which are more uncertain because they assume a prescribed lidar ratio. To begin quantifying the false negative rate relevant to this study, we used two independent methods to estimate the fraction of the time when nighttime Arctic CALIPSO data would not detect above-cloud aerosols when actually present.

Atmos. Chem. Phys. Discuss., doi:10.5194/acp-2016-1037, 2016
Manuscript under review for journal Atmos. Chem. Phys.
Published: 14 December 2016

First, we estimated the fraction of air masses containing various observed concentrations of aerosol tracers that would be detected at the reported theoretical 80 km resolution nighttime backscatter detection limit from Winker et al. (2009). This analysis is based on co-located aircraft backscatter, particle number, and BC data from the ARCTAS aircraft campaign (Fig. 2a). The results suggest that CALIOP would miss ~36% of slightly polluted air masses (i.e., BC concentrations > 30 ng m^{-3}, or CN_{PCASP} concentrations > 127 particles cm^{-3}) at 80 km resolution in nighttime air masses not below another feature (Fig. 2a). This estimate might be affected by errors from assuming Mie theory and a theoretical detection limit that may not be perfectly representative in the field, as well as errors caused by a limited amount of field data from scattered locations.

As an independent consistency check, we next determined the frequency at which aerosols were detected by both FLEXPART and CALIOP. To do so, we compared the fraction of observed clear sky (no-cloud) CALIOP profiles that were expected to contain aerosols at different simulated FLEXPART aerosol concentrations for January 2008 (Fig. 2b). These results suggested that CALIOP may not have detected up to ~33% of slightly polluted air masses (BC > 31 ng m^{-3}) above cloud, although this value likely overestimates the actual false negative rate given inherent model errors. This independent estimate is fairly similar to the previously estimated false negative rate, and so we expect the real-world above-cloud CALIOP false negative rate for dilute aerosols to be ~33-36%. Below-cloud errors would be higher, but are more difficult to quantify because of the variability of in-cloud attenuation.

Based on CALIPSO criteria alone, the above estimates suggest that aerosol detection uncertainties may be higher than desireable, particularly below cloud. Thus, we apply the criteria for determining clean background cloud that depend not only on aerosol-free CALIPSO profiles, but also on modeled above- and below-cloud BC concentrations of < 30 ng m^{-3} (see Sect. 2.1.3). We expect the model aerosol-occurrence criterion to substantially improve the classification confidence because coincidences of false negatives in both the CALIOP data and the model are likely to be rare (they are most likely to occur in dilute aerosol conditions). As such, this method should correctly identify clean background clouds much more frequently than 64-67% of the time. Unfortunately, further quantification in the classification confidence is difficult because both model accuracy and the degree of below-cloud lidar attenuation are variable in time and space. Nonetheless, to our knowledge, the combined CALIPSO and model criteria used here allow the most confident classification of background conditions currently possible for remote sensing studies of the Arctic.

3.2 MOONLiT cloud characteristics in clean marine background conditions

In our study, sampled clouds were thin by definition and were thus unlikely to occur in very turbulent conditions. The range in turbulence covered in the sample set was also likely limited during polar night due to the lower variability in external heating and generally high static stability of the Arctic atmosphere. Nonetheless, we expect that clouds over the open ocean are impacted more by thermodynamic coupling with the surface (Shupe et al., 2013) than over sea ice, where surface-based inversions occur more frequently (Ganeshan and Wu, 2015). In this study, we stratify clouds into these two regimes, to

Atmos. Chem. Phys. Discuss., doi:10.5194/acp-2016-1037, 2016
Manuscript under review for journal Atmos. Chem. Phys.
Published: 14 December 2016

distinguish the effects of systematic differences in atmospheric stability and large-scale atmospheric and surface forcing between the two systems (Curry et al., 1996; Jaiser et al., 2012; Taylor et al., 2015).

MOONLiT clouds over the open ocean were much more likely to overlay another cloud layer (as demonstrated by the average height of the next below-cloud feature, Fig. 3b) than over sea ice (also see Table 2), a result also observed previously at the SHEBA ship-based observatory (Intrieri et al., 2002). As we were only able to analyze upper-layer clouds in this study, the different probability of cloud layering occurring over sea ice and open ocean complicates comparisons between the two regimes. However, comparing only single-layer clouds, it appears that the median cloud base height of open ocean clouds is still ~480 m higher than for clouds over the sea ice ($p < 0.05$, permutation test, Fig. 3c). Interestingly, autumn ship-based cloud observations in the Chukchi and Beaufort Seas also show higher cloud bases over the open ocean [*Sato et al.*, 2012; *Young et al.*, 2016]. The lower cloud heights and the presence of fewer multi-layer MOONLiT clouds over sea ice is likely related to the lower height and greater frequency of surface-based inversions over Arctic sea ice compared to the open ocean, which can reduce surface moisture fluxes to higher altitudes (Bradley et al., 1992; Ganeshan and Wu, 2015; Zhang et al., 2011).

Over the open ocean, clouds were also warmer than over sea ice, and a higher fraction (although not higher total count) of clouds was observed with very low layer mean reflectivity (Z_m), defined as $Z_m < -29$ dBZ (the CloudSat detection limit) (Table 2). The very low Z_m clouds are geometrically and optically very thin and are less likely to be precipitating than the thicker clouds (Table 2). Previous observed relationships between Z_m and r_{el} (Frisch et al., 2002) suggest that the very low Z_m clouds also likely have smaller r_{el} values. Based on the difference between the median estimated cloud r_{el} value in very low Z_m clouds (n=1225) and the median r_{el} for the bottom quartile of clouds with detectable reflectivity (n=306), this difference is estimated to be larger than 1.3 μm. A similar difference (1.1 μm) in clean cloud r_{el} was estimated for open ocean clouds.

Because reflectivity was fairly low within the thin, predominantly liquid cloud profiles that fit our criteria, and temperatures were generally between -7 to -29 ^{o}C, it was difficult to know for certain in many cases which clouds were mixed vs. liquid phase. Of the clouds that were assigned a high-confidence phase classification by CloudSat, most contained some ice particles (100%, n=63 for sea ice, and 93%, n=138 for open ocean). We believe it likely that a comparatively higher fraction of the very low Z_m clouds were present in the liquid-only phase. First, these clouds had very low Z_m values (indicative of small particles), and at the same time they were independently assigned a predominantly liquid phase by CALIPSO. Secondly, their median temperatures were warmer (by ~2^{o}C over sea ice, and nearly 10^{o}C over comparable altitudes over open ocean, see Table S1) than clouds with higher Z_m. Further study would be needed to fully verify phase for this cloud subset, but the indications that these clouds have higher liquid fractions are consistent with the observations that a) Arctic liquid clouds tend to have smaller r_{el} values than mixed-phase clouds (Hobbs and Rangno, 1985; Lance et al., 2011; Lebo et

Atmos. Chem. Phys. Discuss., doi:10.5194/acp-2016-1037, 2016
Manuscript under review for journal Atmos. Chem. Phys.
Published: 14 December 2016

Atmospheric Chemistry and Physics Discussions

al., 2008; Rangno and Hobbs, 2001), and b) clouds over the open ocean (which were more likely to have very low Z_m values (Fig. 4 a,d)) are more likely to be liquid-containing (Cesana et al., 2012).

3.3 Aerosol impacts on clouds over sea ice

We expect that uniformity in surface and meteorological conditions over sea ice will increase the likelihood of being able to isolate aerosol impacts from meteorological noise, compared to the situation over the open ocean, and cloud characteristics were indeed fairly uniform over sea ice. We observed only minor differences in cloud base height between MOONLiT clouds present in clean background conditions and all MOONLiT clouds (Table 2). The cloud base temperatures in clean background conditions were not significantly different from those in all air mass conditions.

Clean background clouds were significantly more likely to be precipitating than other clouds; the likelihood of precipitation based on CloudSat data was respectively 20%, 14%, and 8% for the clean cloud subset, all clouds, and the aerosol-influenced subset. This observation falls in line with aerosol-driven reductions in snowfall that have been predicted and observed previously, inside and outside of the Arctic (Albrecht, 1989; Borys et al., 2000, 2003; Girard et al., 2005; Lance et al., 2011; Lohmann et al., 2003; Mauritsen et al., 2011; Morrison et al., 2008). These observed reductions in precipitation are inconsistent with the glaciation indirect effect, in which ice formation would be expected to increase due to higher concentrations of combustion-related INP (Lohmann and Feichter, 2005).

The presence of aerosols is also correlated with a significant reduction in radar reflectivity, generally associated with smaller particles on theoretical grounds (Fig. 4, Table 2). Although more samples would be needed to explicitly identify any role of meteorological co-variability with radar reflectivity, median cloud temperatures in very low-reflectivity clouds were not significantly different from those in high reflectivity clouds in all conditions over sea ice (Table 2) and there was no noticeable regional clustering of the data that would otherwise suggest that meteorological co-variability was a strong component in this trend (Fig. 1).

The r_{el} values are derived from radar reflectivity, and as such, aerosol-related decreases in reflectivity suggest smaller r_{el} values. This observation follows expectations based on the Twomey effect, and is in line with previous studies in the Arctic that have observed smaller r_{el} correlated with increasing influence of aerosols (Coopman et al., 2016; Lubin and Vogelmann, 2006; Peng et al., 2002; Tietze et al., 2011; Zamora et al., 2016; Zhao and Garrett, 2015). Here, the cloud droplet effective radius decreased systematically as expected aerosol influence rose, and the estimated mode r_{el} was respectively 11.1, 10.2, and 9.9 μm for the clean cloud subset, all clouds, and the aerosol-influenced subset. Unfortunately, the differences in r_{el} are available only for the thicker clouds that CloudSat was able to observe, and in some cases, data were available only for the middle sections of clouds, which are expected to have higher relative r_{el} values. Thus, the estimated mean r_{el} values presented here might be skewed higher than would be derived from a dataset that more fully sampled the cloud fields, and the

Atmos. Chem. Phys. Discuss., doi:10.5194/acp-2016-1037, 2016
Manuscript under review for journal Atmos. Chem. Phys.
Published: 14 December 2016

Atmospheric Chemistry and Physics Discussions

differences compared to clean background cases could underestimate actual differences. Even so, the difference in estimated r_{el} is similar to a previously reported, regionally integrated Arctic value. Using MODIS r_{el} estimates in thicker clouds (median COD ~ 11) with temperatures between 0-2 ^{o}C, Tietze et al. (2011) saw an ~1 μm difference between the very cleanest clouds and median clouds. Note that these regionally averaged net changes in r_{el} are much smaller than would be expected locally in very polluted clouds (e.g., Zamora et al. (2016)).

There are differences between cloud thicknesses in clean background air and other air masses that suggest the potential for meteorological co-variability in the samples. The optical thicknesses of clean background and all MOONLiT clouds are not significantly different, but clean clouds are ~38% thicker than in the subset of aerosol-influenced clouds. Clouds over sea ice that happen to be influenced by aerosols are also geometrically thinner than clean background clouds; median cloud top heights are ~300 m lower (Table 2), resulting in warmer cloud tops. Lower moisture associated with continental airflow that carries the aerosol might explain these differences (Lohmann and Feichter, 2005), if recent surface contact with warmer mostly mid-latitude regions did not enhance moisture. However, in two related remote sensing studies where Arctic clouds were tightly binned within related meteorological groups, COD differences still appeared, and thus the authors attributed these differences to aerosol-driven changes in LWP (Coopman et al., 2016; Tietze et al., 2011).

It is difficult to say whether the aerosol-related impacts on precipitation and radar reflectivity observed here are simply related to Twomey effects on liquid droplets, or whether some more complex mixed-phase and/or meteorological dynamics are also involved. One possibility is that the expected aerosol-driven reductions in r_{el} may hinder the transition from liquid to mixed-phase clouds due to preferential freezing of larger particles (Lohmann and Feichter, 2005; Morrison et al., 2012). One previous aircraft-based study offered some evidence to suggest that the thermodynamic indirect effect is important in the Arctic, particularly for thin clouds (Jackson et al., 2012). However, low sample number and surface/ meteorological variability made this mechanism difficult to conclusively demonstrate on a larger scale. In a different study using CloudSat and CALIPSO, no strong evidence of this process was found (Grenier and Blanchet, 2010). That study was also inconclusive because of high uncertainties related to the reliance on an above-cloud sulfate aerosol proxy, and a focus on ice phase clouds where it is more difficult for CALIPSO to accurately separate aerosols from ice particles. If the very low Z_m clouds in our study do indeed contain fewer cases with ice particles (see Sect. 3.2 above), the greater presence of very low Z_m clouds in aerosol-influenced conditions (Fig. 4) would support the possibility of the thermodynamic indirect effect dominating within the MOONLiT cloud subset. As more information is needed to verify phase in very low Z_m clouds, for now this possibility remains a conjecture.

Other possible mechanisms that could explain the observed aerosol-related impacts on cloud properties are that polluted air might contain fewer ice nucleating particles (INP) than clean background air (Borys, 1989), that solutes might lower the homogeneous freezing temperature and reduce INP efficiency (Girard and Asl, 2014; Koop et al., 1998), that differential

Atmos. Chem. Phys. Discuss., doi:10.5194/acp-2016-1037, 2016
Manuscript under review for journal Atmos. Chem. Phys.
Published: 14 December 2016

Atmospheric Chemistry and Physics Discussions

contact nucleation could play some role (Ladino Moreno et al., 2013; Morrison et al., 2005), and/or that riming efficiency could be reduced (Lohmann and Feichter, 2005).

3.4 Aerosol impacts on clouds over the open ocean

Whereas cloud properties over sea ice were relatively tightly constrained, there was a much larger range in cloud properties over the open ocean (Table 2) that may in part reflect the greater variability and higher magnitudes of surface turbulent heat and moisture fluxes over open ocean (e.g., (Morrison et al., 2008; Strunin et al., 1997; Taylor et al., 2015)). Variability reduced our ability to compare clouds within this regime, as did the uneven vertical distribution of aerosols. CALIPSO-detected aerosols in the Arctic are most frequently found at altitudes below 2 km (Devasthale et al., 2011b; Di Pierro et al., 2013; Kafle and Coulter, 2013; Winker et al., 2013). The median MOONLiT cloud base was above this level over the open ocean (at 2.7 km), and the median cloud base in the clean background cloud subset was even higher (3.3 km). Unsurprisingly, the median base altitude for aerosol-impacted MOONLiT clouds was, in contrast, much closer to this level, at only 2.4 km (Table 2). Thus, the difference in median cloud altitude between the different subsets likely induces a categorical bias in the cloud properties shown in Table 2.

It was quite challenging to both account for aerosol height differences and retain an informative sample size from our 2-year dataset. We separated clouds found over open ocean into three cloud-base-height bins (Table S1), and summarized the resulting information in Table 2. The first bin includes clouds with base heights between 1.0 and 2.6 km. This range encompasses the lower quartile range of all open ocean clouds, and it happens to coincide with the upper quartile range of sea ice clouds (2.5 km), so that these two bins are more or less comparable to each other with respect to cloud-base height. The second bin covers 2.6-4.1 km (the interquartile range of open ocean clouds). The last bin includes clouds with bases > 4.1 km. Although aerosol-influenced clouds still appear most often near the bases of their bins, the median cloud height differences within bins are fairly small (Table S1).

There are significant differences related to aerosols in cloud-base temperature and COD in the full dataset. However, binned differences are inconsistent and not significant, and there are large differences among altitude bins for these parameters. Thus, it is likely that the significant differences in the non-binned COD and base temperature data shown in Table 2 were driven at least in part by altitude bias.

Within and among altitude bins over the open ocean, aerosol-influenced clouds were very slightly thinner, similarly to the samples over the sea ice, but not significantly so. Aerosol-influenced clouds are also less likely to be precipitating, particularly in the lowest bins, but these trends are not significant despite being consistent with the non-binned data and with the sea ice data. Instead, we think it likely that smaller sample size caused the lack of statistical confidence in the binned samples (see Table S1). In contrast to over sea ice, we did not observe a statistically significant aerosol-related reduction in

Atmos. Chem. Phys. Discuss., doi:10.5194/acp-2016-1037, 2016
Manuscript under review for journal Atmos. Chem. Phys.
Published: 14 December 2016

Atmospheric Chemistry and Physics Discussions

r_{el} over open ocean (except in clouds with bases between 2.6-4.1 km). However, the lack of significance across all bins in the dataset used here is not proof of an absence of relationship. In a similar study using MODIS data for liquid clouds over the Arctic, Coopman et al. (2016) did find significant trends in r_{el} with greater predicted aerosol concentrations when they stratified their results by lower tropospheric stability (LTS), which is much greater over sea ice than over open ocean (Taylor et al., 2015). Like us, they found that the trends were weaker for regions with less expected LTS (which in our case would be over open ocean).

Interestingly, for clouds where high quality CloudSat phase information was available, a significantly greater fraction of clouds were assigned a liquid phase in aerosol-influenced samples compared to clean background samples. This trend was significant at the two higher altitude bins over the open ocean; within the lower altitude bin, only one sample was available. It is unclear whether a similar trend in phase would remain if more of the samples had contained high-quality phase data, so we can only remark that the association between aerosols and liquid phase clouds is not inconsistent with the thermodynamic indirect effect.

3.5 Upper bounds on net surface radiative impacts

Over our two-year time period, we identified hundreds of liquid-containing clouds that matched the very strict clean background MOONLiT classification. This sample size and regional spread of the data was large enough that we make the assumption that the MOONLiT cloud characteristics provided in Table 2 approximated the net nighttime cloud characteristics that exist after exposure to the full spectrum of Arctic environmental conditions in each regime (sea ice and open ocean). Cloud patchiness and the presence of lower-level clouds will reduce the regional impact of MOONLiT clouds on the surface. To calculate the *maximum net* radiative impact of clean background MOONLiT clouds on the nighttime surface, we used Table 2 clean background cloud characteristics to calculate longwave flux changes to the surface compared to clear air, assuming cloud homogeneity and a single cloud layer. In these calculations, cloud base height, cloud thickness and COD were taken from the median Table 2 values for all clouds over sea ice and open ocean. In the case of the open ocean, the calculations were then weighted by number of samples in each altitude bin. The interquartile range of r_{el} values was used to reflect the larger uncertainty in that parameter.

The estimated maximum net radiative impact of clean background MOONLiT clouds over sea ice and open ocean during polar night was between 37-40 W m^{-2} over sea ice and 26-28 W m^{-2} over the open ocean. Maximum net MOONLiT cloud impacts on the surface were smaller over the open ocean due to lower temperatures associated with higher median cloud altitudes (an effect also seen during the SHEBA campaign (Shupe and Intrieri, 2004)). Also, the higher open ocean clouds are expected to have lower LWPs (based on thinner CODs, Table 2), which influences longwave cloud forcing in very thin clouds that are not opaque in the infrared (Turner, 2007). If regime differences in cloud cover are taken into account, more realistic maximum net radiative impacts during polar night would be between 19-27 W m^{-2} and 18-24 W m^{-2} over sea ice and

Atmos. Chem. Phys. Discuss., doi:10.5194/acp-2016-1037, 2016
Manuscript under review for journal Atmos. Chem. Phys.
Published: 14 December 2016

Atmospheric Chemistry and Physics Discussions

open ocean regions, respectively, based on a respective 50-70% and a 70-85% cloud cover (Kay and L'Ecuyer, 2013). We expect that real-world net surface impacts over the open ocean will be reduced further relative to sea ice due to the more frequent presence of underlying clouds in that regime (Table 2).

For reference, using the CloudSat 2B-FLEXHR-LIDAR product, Kay and L'Ecuyer (2013) estimated the annual mean LW forcing due to all clouds over sea ice and open ocean to be ~24-36 and 32-56 W m^{-2}, respectively, depending on location. Barton et al. (2014) model-mean estimates for cloud impacts on surface longwave downwelling radiation during polar night over sea ice above 70 ^{o}N (within the 95% confidence interval for surface temperatures) were ~15-30 W m^{-2}. These published estimates included the impacts of non-MOONLiT clouds, which the current study does not.

We also estimated the maximum net surface indirect radiative effect of aerosols on MOONLiT clouds over sea ice. To do so, we subtracted the maximum net surface radiative impacts of the clean background cloud subset from the impacts expected of all observed MOONLiT clouds. Radiative calculations were not made for aerosol-driven effects on MOONLiT clouds over the open ocean due to the lack of significant differences in most relevant parameters and the altitude-based bias in the full open ocean dataset. As with background clouds, aerosol-indirect radiative effect estimates over the sea ice were made using the median cloud base and top heights, the median COD, and the r_{el} interquartile range for sea ice clouds presented in Table 2.

Based on this information, we estimate that excluding changes in cloud fraction, aerosols could have indirectly increased current-day surface downwelling longwave fluxes during polar night over sea ice, from MOONLiT clouds specifically, by no more than 1.1-1.2 W m^{-2}, integrated across the Arctic and for all aerosol concentrations. As with the background cloud estimates, this spatially integrated estimate assumes 100% homogeneous cloud cover and single layer cloud conditions. Based on the same Kay and L'Ecuyer cloud fraction ranges as above, more realistic maximum net changes from aerosols would be ~0.6-0.8 W m^{-2} over sea ice. It is important to note that because this range is spatially integrated across the Arctic, local aerosol impacts in strong haze layers can be much higher (e.g., Garrett et al. (2004); Carrió et al. (2005); Zhao and Garrett (2015)). For example, Zhao and Garrett (2015) found that the local cloud indirect longwave forcing in single-layer stratus clouds at Barrow, Alaska in the upper quartile of combustion aerosol concentrations was 8.1-9.9 W m^{-2} greater than in clouds associated with the lower quartile of combustion aerosol concentrations. In a similar study at Barrow, Lubin and Vogelmann (2006) used the lower and upper quartile of aerosol particle concentrations to show that downwelling flux for high CN cases was 8.2 W m^{-2} higher (3.4 W m^{-2} higher when binned for LWP).

To be clear, in estimating mean aerosol indirect effects in this section, we did not isolate absolute or local indirect aerosol effects from the confounding effects of meteorology and meteorological co-variability. Instead, we estimated the current-day impact of combustion-derived aerosols on the net indirect effect that ultimately influences the current-day surface radiation

Atmos. Chem. Phys. Discuss., doi:10.5194/acp-2016-1037, 2016
Manuscript under review for journal Atmos. Chem. Phys.
Published: 14 December 2016

(which includes any meteorological co-variability present during these two years). This study was limited to only two years of data; future studies with more data might be able to provide a better representation of the full range in aerosol and meteorological conditions the Arctic experiences in the long run.

As a final note, in this study we did not account for any aerosol-driven changes in cloud fraction. Aerosol-driven changes in cloud fraction may have occurred, given the reduced precipitation and the shift in CloudSat-estimated cloud type from predominantly altocumulus to predominantly stratocumulus in increasingly aerosol-impacted conditions over sea ice (Table 2). If aerosols do increase cloud fraction, this effect could be the most important indirect impact that aerosols have on the Arctic's surface radiation budget, because the presence of cloud where there otherwise would not be one has more of a local impact on surface radiation than does a change to a cloud that is already present (Feingold et al., 2016; Sedlar and Devasthale, 2012; Shupe and Intrieri, 2004). Addressing these issues will require further future study with additional types of data.

4 Summary and Conclusions

Aerosol indirect effects have uncertain, but potentially large, impacts on the Arctic energy budget. As a step toward reducing uncertainty in current-day aerosol net indirect effects on the surface, here we have better constrained the characteristics of clean, average and aerosol-impacted clouds. We focused on a commonly observed subset of clouds with bases measured above one km, and that were optically thin (COD<~3), collected at nighttime, predominantly liquid, and were in the top-layer of clouds, termed MOONLiT clouds. For these clouds, it was possible to gain the highest confidence in classification of presence in clean background conditions. Using combined CALIPSO, CloudSat, and model output, we identify clean background MOONLiT clouds with a frequency that is much better than 64-67% of the time. Although the exact frequency of confident identification of clean background conditions beyond this range is difficult to quantify, the level of confidence in clean background classification is a substantial improvement compared to any previous remote sensing study of the Arctic region.

We observed clear differences between clouds over open ocean and over sea ice, consistent with different surface and meteorological conditions between the two regimes. For example, MOONLiT clouds are nearly twice as likely to overlay another cloud when the surface is open ocean compared to sea ice, and are more likely to be present in liquid phase. A greater frequency of multi-layer clouds over the open ocean might affect how the retreat of sea ice changes the impact of clouds on surface radiation of the Arctic Ocean. However, further study is needed to expand this observation beyond just conditions that contain MOONLiT clouds.

MOONLiT clouds are susceptible to aerosols, and likely have an effect on surface radiation. Consistent with other studies, the presence of aerosols in clouds over sea ice is associated with reductions in r_{el}, cloud geometric and optical thickness,

Atmos. Chem. Phys. Discuss., doi:10.5194/acp-2016-1037, 2016
Manuscript under review for journal Atmos. Chem. Phys.
Published: 14 December 2016

Atmospheric Chemistry and Physics Discussions

precipitation, radar reflectivity, and COD. Perhaps due to greater boundary layer turbulent fluxes, clouds over the open ocean appear to be less susceptible to the influence of aerosols, although some changes in phase and thickness were observed in the altitude binned samples presented here. Due to aerosol-induced MOONLiT cloud changes over sea ice, we estimate that the regional-scale maximum net surface radiation impact during polar night is ~0.6-0.8 W m^{-2}. It is unclear from the current work what the impact over open ocean might be. In comparison, the maximum net direct radiative impact of clean MOONLiT clouds at night is estimated to be between 19-27 W m^{-2} and 18-24 W m^{-2} over sea ice and open ocean regions, respectively. Note that the presence of multi-layer clouds and cloud patchiness will reduce the radiative impact of MOONLiT clouds on the surface. Also, these maximum net indirect effect estimates do not include any potential aerosol-driven changes in cloud extent, which could be important for estimating the overall net indirect effects. Thus, aerosol-driven changes in cloud fraction dominate the uncertainty in estimates of the overall indirect aerosol radiative impact on the nighttime Arctic surface energy balance, based on this method. Unfortunately, the cloud fraction in the Arctic is particularly difficult to constrain over short time scales with remote sensing, given the low contrast between clouds and sea ice and long polar nighttime conditions.

We find evidence to suggest that the glaciation indirect effect is not important within the MOONLiT cloud subset. Beyond that, we have no strong support for aerosol impacts on mixed-phase cloud dynamics, although we see some tantalizing evidence to suggest that large liquid particles need be present for ice formation in MOONLiT clouds, in a mechanism similar to the thermodynamic indirect effect. These findings are in line with and expand upon previous aircraft observations (Jackson et al., 2012). Compared to clouds with higher radar reflectivity, very low Z_m clouds in clean background conditions were thinner. Clouds influenced by aerosol were also less likely to be precipitating, less reflective at 94-GHz, and had estimated median r_{el} values that were noticeably smaller, which is also in line with previous studies. Over the open ocean, aerosols were associated with higher fractions of liquid phase clouds than in clean background cases. Together, these observations suggest that aerosols could play an important role in ice nucleation and nighttime radiative heating via the thermodynamic indirect effect in MOONLiT clouds. However, more information on cloud phase in low-reflectivity clouds is necessary to more fully explore this possibility.

This study was limited to only MOONLiT clouds present in specified conditions where it was most possible to identify the presence of aerosols. To constrain observation-based net aerosol impacts and nucleation processes on a larger scale, optically thick clouds, predominantly ice-containing clouds, and clouds below the upper layer must be included. One would also want to include clouds with bases < 1 km, which are very common and have a high exposure to aerosols. Expanding the study to include daylit or summertime air masses would be useful; mid-summer air masses tend to be cleaner than wintertime Arctic air masses and have a higher fraction of liquid-containing clouds (Van Tricht et al., 2016). Moreover, it would enable the use of MODIS data to examine cloud phase (e.g., via the DARDAR data product (Delanoë and Hogan, 2010)) and droplet distribution. Expanding this study to a longer time period would help better incorporate the natural variability in Arctic

meteorology and aerosols that might not be represented during this 2-year period.

Although we limited this study to carefully describing average and clean background clouds within only a subset of remotely sensed Arctic clouds, we were able to provide a first observation-based estimate of regional scale net aerosol indirect effects on the surface for such clouds. Therefore, given that so far only models have been able to estimate net aerosol indirect effects on the surface energy balance, this study lays a foundation for improving the quantification of aerosol indirect effects. Future studies that include other cloud types, over longer time periods, could provide more comprehensive observational constraints on these effects.

Acknowledgements

We recognize and thank the efforts and funding from the large number of people and agencies involved in making the following datasets available, including: the NASA Langley Research Center Atmospheric Science Data Center, which provided the CALIPSO data, and the NASA ARCTAS program and members. Specifically we would like to thank Y. Kondo and B. Anderson for making their ARCTAS data publically available. We also thank G. de Boer, J. Creamean, G. Feingold, K.B. Huebert, J. Limbacher, R. Moore, A. Solomon, H. Telg, M. Vaughan, D.L. Wu, Y. Yang, H. Yu, and T.L. Yuan for helpful discussions. The research of L. Zamora was supported by the NASA ACMAP program, via an appointment to the NASA Postdoctoral Program at the NASA Goddard Space Flight Center, administered by Universities Space Research Association. The work of R. Kahn is supported in part by NASA's Climate and Radiation Research and Analysis Program under H. Maring, and NASA's Atmospheric Composition Program under R. Eckman. The NILU team was supported by funding from NordForsk in the framework of eSTICC (eScience Tools for Investigating Climate Change at High Northern Latitudes).

Atmos. Chem. Phys. Discuss., doi:10.5194/acp-2016-1037, 2016
Manuscript under review for journal Atmos. Chem. Phys.
Published: 14 December 2016

Atmospheric Chemistry and Physics Discussions

Appendix A

In Zamora et al. (2016), the case study CODs were not presented. Here, we calculated the relevant CODs from the following relationship:

$$(2)\quad COD = \frac{3}{2}\frac{LWC\ (z_t - z_b)}{r_{el}},$$

where LWC is the liquid water content, z_t and z_b are cloud top and base height, respectively, and r_{el} is the cloud droplet effective radius.

Supplement link (to be provided by Copernicus)

Competing Interests:

The authors declare that they have no conflict of interest.

References

Albrecht, B. A.: Aerosols, Cloud Microphysics, and Fractional Cloudiness, Science, 245(4923), 1227–1230, doi:10.1126/science.245.4923.1227, 1989.

Amante, C. and Eakins, B. W.: ETOPO1 1 Arc-Minute Global Relief Model: Procedures, Data Sources and Analysis. NOAA Technical Memorandum NESDIS NGDC-24. National Geophysical Data Center, NOAA., , doi:10.7289/V5C8276M, 2009.

Anderson, T. L. and Ogren, J. A.: Determining Aerosol Radiative Properties Using the TSI 3563 Integrating Nephelometer, Aerosol Sci. Technol., 29(1), 57–69, doi:10.1080/02786829808965551, 1998.

Austin, R. T. and Stephens, G. L.: Retrieval of stratus cloud microphysical parameters using millimeter-wave radar and visible optical depth in preparation for CloudSat: 1. Algorithm formulation, J. Geophys. Res. Atmospheres, 106(D22), 28233–28242, doi:10.1029/2000JD000293, 2001.

Barton, N. P., Klein, S. A. and Boyle, J. S.: On the Contribution of Longwave Radiation to Global Climate Model Biases in Arctic Lower Tropospheric Stability, J. Clim., 27(19), 7250–7269, doi:10.1175/JCLI-D-14-00126.1, 2014.

Bennartz, R., Shupe, M. D., Turner, D. D., Walden, V. P., Steffen, K., Cox, C. J., Kulie, M. S., Miller, N. B. and Pettersen, C.: July 2012 Greenland melt extent enhanced by low-level liquid clouds, Nature, 496(7443), 83–86, doi:10.1038/nature12002, 2013.

de Boer, G., Tripoli, G. J. and Eloranta, E. W.: Preliminary comparison of CloudSAT-derived microphysical quantities with ground-based measurements for mixed-phase cloud research in the Arctic, J. Geophys. Res. Atmospheres, 113(D8), D00A06, doi:10.1029/2008JD010029, 2008.

Borys, R. D.: Studies of ice nucleation by Arctic aerosol on AGASP-II, J. Atmospheric Chem., 9(1–3), 169–185, doi:10.1007/BF00052831, 1989.

Borys, R. D., Lowenthal, D. H. and Mitchell, D. L.: The relationships among cloud microphysics, chemistry, and precipitation rate in cold mountain clouds, Atmos. Environ., 34(16), 2593–2602, doi:10.1016/S1352-2310(99)00492-6, 2000.

Borys, R. D., Lowenthal, D. H., Cohn, S. A. and Brown, W. O. J.: Mountaintop and radar measurements of anthropogenic aerosol effects on snow growth and snowfall rate, Geophys. Res. Lett., 30(10), 1538, doi:10.1029/2002GL016855, 2003.

Boucher, O., Randall, D. A., Artaxo, P., Bretherton, C. S., Feingold, G., Forster, P. M., Kerminen, V.-M., Kondo, Y., Liao, H., Lohmann, U., Rasch, P., Satheesh, S. K., Sherwood, S., Stevens, B. and Zhang, X. Y.: Clouds and Aerosols, in Climate

Change 2013: The Physical Science Basis. Contribution of Working Group I to the Fifth Assessment Report of the Intergovernmental Panel on Climate Change, edited by T. F. Stocker, D. Qin, G. K. Plattner, M. Tignor, S. K. Allen, J. Boschung, A. Nauels, Y. Xia, V. Bex, and P. M. Midgley, Cambridge University Press, Cambridge, UK and New York, NY, USA., 2013.

Bradley, R. S., Keimig, F. T. and Diaz, H. F.: Climatology of surface-based inversions in the North American Arctic, J. Geophys. Res. Atmospheres, 97(D14), 15699–15712, doi:10.1029/92JD01451, 1992.

Carrió, G. G., Jiang, H. and Cotton, W. R.: Impact of Aerosol Intrusions on Arctic Boundary Layer Clouds. Part II: Sea Ice Melting Rates, J. Atmospheric Sci., 62(9), 3094–3105, doi:10.1175/JAS3558.1, 2005.

Cesana, G., Kay, J. E., Chepfer, H., English, J. M. and Boer, G. de: Ubiquitous low-level liquid-containing Arctic clouds: New observations and climate model constraints from CALIPSO-GOCCP, Geophys. Res. Lett., 39(20), L20804, doi:10.1029/2012GL053385, 2012.

Chakrabarty, R. K., Gyawali, M., Yatavelli, R. L. N., Pandey, A., Watts, A. C., Knue, J., Chen, L.-W. A., Pattison, R. R., Tsibart, A., Samburova, V. and Moosmüller, H.: Brown carbon aerosols from burning of boreal peatlands: microphysical properties, emission factors, and implications for direct radiative forcing, Atmos Chem Phys, 16(5), 3033–3040, doi:10.5194/acp-16-3033-2016, 2016.

Christensen, M. W., Stephens, G. L. and Lebsock, M. D.: Exposing biases in retrieved low cloud properties from CloudSat: A guide for evaluating observations and climate data, J. Geophys. Res. Atmospheres, 118(21), 12,120-12,131, doi:10.1002/2013JD020224, 2013.

Coopman, Q., Garrett, T. J., Riedi, J., Eckhardt, S. and Stohl, A.: Effects of long-range aerosol transport on the microphysical properties of low-level liquid clouds in the Arctic, Atmos Chem Phys, 16(7), 4661–4674, doi:10.5194/acp-16-4661-2016, 2016.

Curry, J. A., Schramm, J. L., Rossow, W. B. and Randall, D.: Overview of Arctic Cloud and Radiation Characteristics, J. Clim., 9(8), 1731–1764, doi:10.1175/1520-0442(1996)009<1731:OOACAR>2.0.CO;2, 1996.

Damoah, R., Spichtinger, N., Forster, C., James, P., Mattis, I., Wandinger, U., Beirle, S., Wagner, T. and Stohl, A.: Around the world in 17 days - hemispheric-scale transport of forest fire smoke from Russia in May 2003, Atmos Chem Phys, 4(5), 1311–1321, doi:10.5194/acp-4-1311-2004, 2004.

Delanoë, J. and Hogan, R. J.: Combined CloudSat-CALIPSO-MODIS retrievals of the properties of ice clouds, J. Geophys. Res. Atmospheres, 115(D4), D00H29, doi:10.1029/2009JD012346, 2010.

Devasthale, A., TjernströM, M., Karlsson, K.-G., Thomas, M. A., Jones, C., Sedlar, J. and Omar, A. H.: The vertical distribution of thin features over the Arctic analysed from CALIPSO observations, Part I: Optically thin clouds, Tellus B, 63(1), 77–85, doi:10.1111/j.1600-0889.2010.00516.x, 2011a.

Devasthale, A., Tjernström, M. and Omar, A. H.: The vertical distribution of thin features over the Arctic analysed from CALIPSO observations. Part II: Aerosols, Tellus B, 63(1), doi:10.3402/tellusb.v63i1.16190, 2011b.

Di Pierro, M., Jaeglé, L., Eloranta, E. W. and Sharma, S.: Spatial and seasonal distribution of Arctic aerosols observed by the CALIOP satellite instrument (2006–2012), Atmos Chem Phys, 13(14), 7075–7095, doi:10.5194/acp-13-7075-2013, 2013.

Eckhardt, S., Quennehen, B., Olivié, D. J. L., Berntsen, T. K., Cherian, R., Christensen, J. H., Collins, W., Crepinsek, S., Daskalakis, N., Flanner, M., Herber, A., Heyes, C., Hodnebrog, Ø., Huang, L., Kanakidou, M., Klimont, Z., Langner, J., Law, K. S., Lund, M. T., Mahmood, R., Massling, A., Myriokefalitakis, S., Nielsen, I. E., Nøjgaard, J. K., Quaas, J., Quinn, P. K., Raut, J.-C., Rumbold, S. T., Schulz, M., Sharma, S., Skeie, R. B., Skov, H., Uttal, T., von Salzen, K. and Stohl, A.: Current model capabilities for simulating black carbon and sulfate concentrations in the Arctic atmosphere: a multi-model evaluation using a comprehensive measurement data set, Atmos Chem Phys, 15(16), 9413–9433, doi:10.5194/acp-15-9413-2015, 2015.

Feingold, G., McComiskey, A., Yamaguchi, T., Johnson, J. S., Carslaw, K. S. and Schmidt, K. S.: New approaches to quantifying aerosol influence on the cloud radiative effect, Proc. Natl. Acad. Sci., 201514035, doi:10.1073/pnas.1514035112, 2016.

Forster, C., Wandinger, U., Wotawa, G., James, P., Mattis, I., Althausen, D., Simmonds, P., O'Doherty, S., Jennings, S. G., Kleefeld, C., Schneider, J., Trickl, T., Kreipl, S., Jäger, H. and Stohl, A.: Transport of boreal forest fire emissions from Canada to Europe, J. Geophys. Res. Atmospheres, 106(D19), 22887–22906, doi:10.1029/2001JD900115, 2001.

Frisch, S., Shupe, M., Djalalova, I., Feingold, G. and Poellot, M.: The Retrieval of Stratus Cloud Droplet Effective Radius with Cloud Radars, J. Atmospheric Ocean. Technol., 19(6), 835–842, doi:10.1175/1520-0426(2002)019<0835:TROSCD>2.0.CO;2, 2002.

Fuelberg, H. E., Harrigan, D. L. and Sessions, W.: A meteorological overview of the ARCTAS 2008 mission, Atmos Chem Phys, 10(2), 817–842, doi:10.5194/acp-10-817-2010, 2010.

Ganeshan, M. and Wu, D. L.: An investigation of the Arctic inversion using COSMIC RO observations, J. Geophys. Res. Atmospheres, 120(18), 2015JD023058, doi:10.1002/2015JD023058, 2015.

Garrett, T. J. and Zhao, C.: Increased Arctic cloud longwave emissivity associated with pollution from mid-latitudes, Nature, 440(7085), 787–789, doi:10.1038/nature04636, 2006.

Garrett, T. J., Zhao, C., Dong, X., Mace, G. G. and Hobbs, P. V.: Effects of varying aerosol regimes on low-level Arctic stratus, Geophys. Res. Lett., 31(17), L17105, doi:10.1029/2004GL019928, 2004.

Ghan, S., Wang, M., Zhang, S., Ferrachat, S., Gettelman, A., Griesfeller, J., Kipling, Z., Lohmann, U., Morrison, H., Neubauer, D., Partridge, D. G., Stier, P., Takemura, T., Wang, H. and Zhang, K.: Challenges in constraining anthropogenic aerosol effects on cloud radiative forcing using present-day spatiotemporal variability, Proc. Natl. Acad. Sci., 201514036, doi:10.1073/pnas.1514036113, 2016.

Girard, E. and Asl, N. S.: Relative importance of acid coating on ice nuclei in the deposition and contact modes for wintertime Arctic clouds and radiation, Meteorol. Atmospheric Phys., 123(1–2), 81–92, doi:10.1007/s00703-013-0298-9, 2014.

Girard, E., Blanchet, J.-P. and Dubois, Y.: Effects of arctic sulphuric acid aerosols on wintertime low-level atmospheric ice crystals, humidity and temperature at Alert, Nunavut, Atmospheric Res., 73(1–2), 131–148, doi:10.1016/j.atmosres.2004.08.002, 2005.

Girard, E., Dueymes, G., Du, P. and Bertram, A. K.: Assessment of the effects of acid-coated ice nuclei on the Arctic cloud microstructure, atmospheric dehydration, radiation and temperature during winter, Int. J. Climatol., 33(3), 599–614, doi:10.1002/joc.3454, 2013.

GMAO: MERRA-2 tavgM_2d_rad_Nx: 2d,Monthly mean,Time-Averaged,Single-Level,Assimilation,Radiation Diagnostics V5.12.4, version 5.12.4, Greenbelt, MD, USA, Goddard Earth Sciences Data and Information Services Center (GES DISC), Accessed June 20, 2016, , doi:10.5067/OU3HJDS973O0, 2015.

Grenier, P. and Blanchet, J.-P.: Investigation of the sulphate-induced freezing inhibition effect from CloudSat and CALIPSO measurements, J. Geophys. Res. Atmospheres, 115(D22), D22205, doi:10.1029/2010JD013905, 2010.

Hamilton, D. S., Lee, L. A., Pringle, K. J., Reddington, C. L., Spracklen, D. V. and Carslaw, K. S.: Occurrence of pristine aerosol environments on a polluted planet, Proc. Natl. Acad. Sci., 111(52), 18466–18471, doi:10.1073/pnas.1415440111, 2014.

Hobbs, P. V. and Rangno, A. L.: Ice Particle Concentrations in Clouds, J. Atmospheric Sci., 42(23), 2523–2549, doi:10.1175/1520-0469(1985)042<2523:IPCIC>2.0.CO;2, 1985.

Huang, Y., Siems, S. T., Manton, M. J., Protat, A. and Delanoë, J.: A study on the low-altitude clouds over the Southern Ocean using the DARDAR-MASK, J. Geophys. Res. Atmospheres, 117(D18), D18204, doi:10.1029/2012JD017800, 2012.

Intrieri, J. M., Shupe, M. D., Uttal, T. and McCarty, B. J.: An annual cycle of Arctic cloud characteristics observed by radar and lidar at SHEBA, J. Geophys. Res. Oceans, 107(C10), SHE 5-1, doi:10.1029/2000JC000423, 2002.

Jackson, R. C., McFarquhar, G. M., Korolev, A. V., Earle, M. E., Liu, P. S. K., Lawson, R. P., Brooks, S., Wolde, M., Laskin, A. and Freer, M.: The dependence of ice microphysics on aerosol concentration in arctic mixed-phase stratus clouds during ISDAC and M-PACE, J. Geophys. Res., 117(D15), D15207, doi:10.1029/2012JD017668, 2012.

Jacob, D. J., Crawford, J. H., Maring, H., Clarke, A. D., Dibb, J. E., Emmons, L. K., Ferrare, R. A., Hostetler, C. A., Russell, P. B., Singh, H. B., Thompson, A. M., Shaw, G. E., McCauley, E., Pederson, J. R. and Fisher, J. A.: The Arctic Research of the Composition of the Troposphere from Aircraft and Satellites (ARCTAS) mission: design, execution, and first results, Atmos Chem Phys, 10(11), 5191–5212, doi:10.5194/acp-10-5191-2010, 2010.

Jaiser, R., Dethloff, K., Handorf, D., Rinke, A. and Cohen, J.: Impact of sea ice cover changes on the Northern Hemisphere atmospheric winter circulation, Tellus A, 64(0), doi:10.3402/tellusa.v64i0.11595, 2012.

Jiao, C. and Flanner, M. G.: Changing black carbon transport to the Arctic from present day to the end of 21st century, J. Geophys. Res. Atmospheres, 121(9), 2015JD023964, doi:10.1002/2015JD023964, 2016.

Josey, S. A.: Changes in the heat and freshwater forcing of the eastern Mediterranean and their influence on deep water formation, J. Geophys. Res. Oceans, 108(C7), 3237, doi:10.1029/2003JC001778, 2003.

Kacenelenbogen, M., Redemann, J., Vaughan, M. A., Omar, A. H., Russell, P. B., Burton, S., Rogers, R. R., Ferrare, R. A. and Hostetler, C. A.: An evaluation of CALIOP/CALIPSO's aerosol-above-cloud detection and retrieval capability over North America, J. Geophys. Res. Atmospheres, 119(1), 230–244, doi:10.1002/2013JD020178, 2014.

Kafle, D. N. and Coulter, R. L.: Micropulse lidar-derived aerosol optical depth climatology at ARM sites worldwide, J. Geophys. Res. Atmospheres, 118(13), 7293–7308, doi:10.1002/jgrd.50536, 2013.

Kay, J. E. and L'Ecuyer, T.: Observational constraints on Arctic Ocean clouds and radiative fluxes during the early 21st century, J. Geophys. Res. Atmospheres, 118(13), 7219–7236, doi:10.1002/jgrd.50489, 2013.

Kondo, Y., Matsui, H., Moteki, N., Sahu, L., Takegawa, N., Kajino, M., Zhao, Y., Cubison, M. J., Jimenez, J. L., Vay, S., Diskin, G. S., Anderson, B., Wisthaler, A., Mikoviny, T., Fuelberg, H. E., Blake, D. R., Huey, G., Weinheimer, A. J., Knapp, D. J. and Brune, W. H.: Emissions of black carbon, organic, and inorganic aerosols from biomass burning in North America and Asia in 2008, J. Geophys. Res. Atmospheres, 116(D8), D08204, doi:10.1029/2010JD015152, 2011.

Koop, T., Ng, H. P., Molina, L. T. and Molina, M. J.: A New Optical Technique to Study Aerosol Phase Transitions: The Nucleation of Ice from H2SO4 Aerosols, J. Phys. Chem. A, 102(45), 8924–8931, doi:10.1021/jp9828078, 1998.

Ladino Moreno, L. A., Stetzer, O. and Lohmann, U.: Contact freezing: a review of experimental studies, Atmos Chem Phys, 13(19), 9745–9769, doi:10.5194/acp-13-9745-2013, 2013.

Lance, S., Shupe, M. D., Feingold, G., Brock, C. A., Cozic, J., Holloway, J. S., Moore, R. H., Nenes, A., Schwarz, J. P., Spackman, J. R., Froyd, K. D., Murphy, D. M., Brioude, J., Cooper, O. R., Stohl, A. and Burkhart, J. F.: Cloud condensation nuclei as a modulator of ice processes in Arctic mixed-phase clouds, Atmospheric Chem. Phys., 11(15), 8003–8015, 2011.

Lebo, Z. J., Johnson, N. C. and Harrington, J. Y.: Radiative influences on ice crystal and droplet growth within mixed-phase stratus clouds, J. Geophys. Res. Atmospheres, 113(D9), D09203, doi:10.1029/2007JD009262, 2008.

Lee, S., Kahn, B. H. and Teixeira, J.: Characterization of cloud liquid water content distributions from CloudSat, J. Geophys. Res. Atmospheres, 115(D20), D20203, doi:10.1029/2009JD013272, 2010.

Liu, Z., Vaughan, M., Winker, D., Kittaka, C., Getzewich, B., Kuehn, R., Omar, A., Powell, K., Trepte, C. and Hostetler, C.: The CALIPSO Lidar Cloud and Aerosol Discrimination: Version 2 Algorithm and Initial Assessment of Performance, J. Atmospheric Ocean. Technol., 26(7), 1198–1213, doi:10.1175/2009JTECHA1229.1, 2009.

Lohmann, U. and Feichter, J.: Global indirect aerosol effects: a review, Atmos Chem Phys, 5(3), 715–737, doi:10.5194/acp-5-715-2005, 2005.

Lohmann, U., Zhang, J. and Pi, J.: Sensitivity studies of the effect of increased aerosol concentrations and snow crystal shape on the snowfall rate in the Arctic, J. Geophys. Res. Atmospheres, 108(D11), 4341, doi:10.1029/2003JD003377, 2003.

Lubin, D. and Vogelmann, A. M.: A climatologically significant aerosol longwave indirect effect in the Arctic, Nature, 439(7075), 453–456, doi:10.1038/nature04449, 2006.

Mauritsen, T., Sedlar, J., Tjernström, M., Leck, C., Martin, M., Shupe, M., Sjogren, S., Sierau, B., Persson, P. O. G., Brooks, I. M. and Swietlicki, E.: An Arctic CCN-limited cloud-aerosol regime, Atmos Chem Phys, 11(1), 165–173, doi:10.5194/acp-11-165-2011, 2011.

McComiskey, A. and Feingold, G.: Quantifying error in the radiative forcing of the first aerosol indirect effect, Geophys. Res. Lett., 35(2), L02810, doi:10.1029/2007GL032667, 2008.

Meier, W., Fetterer, F., Savoie, M., Mallory, S., Duerr, R. and Stroeve, J. C.: NOAA/NSIDC Climate Data Record of Passive Microwave Sea Ice Concentration, Version 2. [G02202], NSIDC: National Snow and Ice Data Center, Boulder, Colorado, USA. [online] Available from: doi: http://dx.doi.org/10.7265/N55M63M1 (Accessed 23 May 2016), 2013.

Mioche, G., Jourdan, O., Ceccaldi, M. and Delanoë, J.: Variability of mixed-phase clouds in the Arctic with a focus on the Svalbard region: a study based on spaceborne active remote sensing, Atmos Chem Phys, 15(5), 2445–2461, doi:10.5194/acp-15-2445-2015, 2015.

Morrison, H., Shupe, M. D., Pinto, J. O. and Curry, J. A.: Possible roles of ice nucleation mode and ice nuclei depletion in the extended lifetime of Arctic mixed-phase clouds, Geophys. Res. Lett., 32(18), L18801, doi:10.1029/2005GL023614, 2005.

Morrison, H., Pinto, J. O., Curry, J. A. and McFarquhar, G. M.: Sensitivity of modeled arctic mixed-phase stratocumulus to cloud condensation and ice nuclei over regionally varying surface conditions, J. Geophys. Res. Atmospheres, 113(D5), D05203, doi:10.1029/2007JD008729, 2008.

Morrison, H., de Boer, G., Feingold, G., Harrington, J., Shupe, M. D. and Sulia, K.: Resilience of persistent Arctic mixed-phase clouds, Nat. Geosci., 5(1), 11–17, doi:10.1038/ngeo1332, 2012.

Ovchinnikov, M., Ackerman, A. S., Avramov, A., Cheng, A., Fan, J., Fridlind, A. M., Ghan, S., Harrington, J., Hoose, C., Korolev, A., McFarquhar, G. M., Morrison, H., Paukert, M., Savre, J., Shipway, B. J., Shupe, M. D., Solomon, A. and Sulia, K.: Intercomparison of large-eddy simulations of Arctic mixed-phase clouds: Importance of ice size distribution assumptions, J. Adv. Model. Earth Syst., 6(1), 223–248, doi:10.1002/2013MS000282, 2014.

Paris, J.-D., Stohl, A., Nédélec, P., Arshinov, M. Y., Panchenko, M. V., Shmargunov, V. P., Law, K. S., Belan, B. D. and Ciais, P.: Wildfire smoke in the Siberian Arctic in summer: source characterization and plume evolution from airborne measurements, Atmos Chem Phys, 9(23), 9315–9327, doi:10.5194/acp-9-9315-2009, 2009.

Peng, G., Meier, W. N., Scott, D. J. and Savoie, M. H.: A long-term and reproducible passive microwave sea ice concentration data record for climate studies and monitoring, Earth Syst. Sci. Data, 5(2), 311–318, doi:10.5194/essd-5-311-2013, 2013.

Peng, Y., Lohmann, U., Leaitch, R., Banic, C. and Couture, M.: The cloud albedo-cloud droplet effective radius relationship for clean and polluted clouds from RACE and FIRE.ACE, J. Geophys. Res. Atmospheres, 107(D11), AAC 1-1, doi:10.1029/2000JD000281, 2002.

Rangno, A. L. and Hobbs, P. V.: Ice particles in stratiform clouds in the Arctic and possible mechanisms for the production of high ice concentrations, J. Geophys. Res. Atmospheres, 106(D14), 15065–15075, doi:10.1029/2000JD900286, 2001.

Ricchiazzi, P., Yang, S., Gautier, C. and Sowle, D.: SBDART: A Research and Teaching Software Tool for Plane-Parallel Radiative Transfer in the Earth's Atmosphere, Bull. Am. Meteorol. Soc., 79(10), 2101–2114, doi:10.1175/1520-0477(1998)079<2101:SARATS>2.0.CO;2, 1998.

Rogers, R. R., Vaughan, M. A., Hostetler, C. A., Burton, S. P., Ferrare, R. A., Young, S. A., Hair, J. W., Obland, M. D., Harper, D. B., Cook, A. L. and Winker, D. M.: Looking through the haze: evaluating the CALIPSO level 2 aerosol optical depth using airborne high spectral resolution lidar data, Atmos Meas Tech, 7(12), 4317–4340, doi:10.5194/amt-7-4317-2014, 2014.

Sedlar, J. and Devasthale, A.: Clear-sky thermodynamic and radiative anomalies over a sea ice sensitive region of the Arctic, J. Geophys. Res., 117(D19), doi:10.1029/2012JD017754, 2012.

Serreze, M. C., Barrett, A. P., Stroeve, J. C., Kindig, D. N. and Holland, M. M.: The emergence of surface-based Arctic amplification, The Cryosphere, 3(1), 11–19, doi:10.5194/tc-3-11-2009, 2009.

Shaw, G. E.: The Arctic Haze Phenomenon, Bull. Am. Meteorol. Soc., 76(12), 2403–2413, doi:10.1175/1520-0477(1995)076<2403:TAHP>2.0.CO;2, 1995.

Sheridan, P. J., Andrews, E., Ogren, J. A., Tackett, J. L. and Winker, D. M.: Vertical profiles of aerosol optical properties over central Illinois and comparison with surface and satellite measurements, Atmos Chem Phys, 12(23), 11695–11721, doi:10.5194/acp-12-11695-2012, 2012.

Shupe, M. D. and Intrieri, J. M.: Cloud Radiative Forcing of the Arctic Surface: The Influence of Cloud Properties, Surface Albedo, and Solar Zenith Angle, J. Clim., 17(3), 616–628, doi:10.1175/1520-0442(2004)017<0616:CRFOTA>2.0.CO;2, 2004.

Shupe, M. D., Walden, V. P., Eloranta, E., Uttal, T., Campbell, J. R., Starkweather, S. M. and Shiobara, M.: Clouds at Arctic Atmospheric Observatories. Part I: Occurrence and Macrophysical Properties, J. Appl. Meteorol. Climatol., 50(3), 626–644, doi:10.1175/2010JAMC2467.1, 2011.

Shupe, M. D., Persson, P. O. G., Brooks, I. M., Tjernström, M., Sedlar, J., Mauritsen, T., Sjogren, S. and Leck, C.: Cloud and boundary layer interactions over the Arctic sea ice in late summer, Atmos Chem Phys, 13(18), 9379–9399, doi:10.5194/acp-13-9379-2013, 2013.

Sodemann, H., Pommier, M., Arnold, S. R., Monks, S. A., Stebel, K., Burkhart, J. F., Hair, J. W., Diskin, G. S., Clerbaux, C., Coheur, P.-F., Hurtmans, D., Schlager, H., Blechschmidt, A.-M., Kristjánsson, J. E. and Stohl, A.: Episodes of cross-polar transport in the Arctic troposphere during July 2008 as seen from models, satellite, and aircraft observations, Atmos Chem Phys, 11(8), 3631–3651, doi:10.5194/acp-11-3631-2011, 2011.

Stohl, A., Hittenberger, M. and Wotawa, G.: Validation of the lagrangian particle dispersion model FLEXPART against large-scale tracer experiment data, Atmos. Environ., 32(24), 4245–4264, doi:10.1016/S1352-2310(98)00184-8, 1998.

Stohl, A., Eckhardt, S., Forster, C., James, P. and Spichtinger, N.: On the pathways and timescales of intercontinental air pollution transport, J. Geophys. Res. Atmospheres, 107(D23), 4684, doi:10.1029/2001JD001396, 2002.

Stohl, A., Forster, C., Eckhardt, S., Spichtinger, N., Huntrieser, H., Heland, J., Schlager, H., Wilhelm, S., Arnold, F. and Cooper, O.: A backward modeling study of intercontinental pollution transport using aircraft measurements, J. Geophys. Res. Atmospheres, 108(D12), 4370, doi:10.1029/2002JD002862, 2003.

Stohl, A., Forster, C., Frank, A., Seibert, P. and Wotawa, G.: Technical note: The Lagrangian particle dispersion model FLEXPART version 6.2, Atmos Chem Phys, 5(9), 2461–2474, doi:10.5194/acp-5-2461-2005, 2005.

Stohl, A., Aamaas, B., Amann, M., Baker, L. H., Bellouin, N., Berntsen, T. K., Boucher, O., Cherian, R., Collins, W., Daskalakis, N., Dusinska, M., Eckhardt, S., Fuglestvedt, J. S., Harju, M., Heyes, C., Hodnebrog, Ø., Hao, J., Im, U., Kanakidou, M., Klimont, Z., Kupiainen, K., Law, K. S., Lund, M. T., Maas, R., MacIntosh, C. R., Myhre, G., Myriokefalitakis, S., Olivié, D., Quaas, J., Quennehen, B., Raut, J.-C., Rumbold, S. T., Samset, B. H., Schulz, M., Seland, Ø., Shine, K. P., Skeie, R. B., Wang, S., Yttri, K. E. and Zhu, T.: Evaluating the climate and air quality impacts of short-lived pollutants, Atmos Chem Phys, 15(18), 10529–10566, doi:10.5194/acp-15-10529-2015, 2015.

Strunin, M. A., Postnov, A. A. and Mezrin, M. Y.: Arctic HazeMeteorological potential for contamination of arctic troposphere: Boundary layer structure and turbulent diffusion characteristics, Atmospheric Res., 44(1), 37–51, doi:10.1016/S0169-8095(97)00008-2, 1997.

Taylor, P. C., Kato, S., Xu, K.-M. and Cai, M.: Covariance between Arctic sea ice and clouds within atmospheric state regimes at the satellite footprint level, J. Geophys. Res. Atmospheres, 120(24), 2015JD023520, doi:10.1002/2015JD023520, 2015.

Tietze, K., Riedi, J., Stohl, A. and Garret, T. J.: Space-based evaluation of interactions between aerosols and low-level Arctic clouds during the Spring and Summer of 2008, Atmospheric Chem. Phys., 11, 3359–3373, NaN-11-3359–2011, 2011.

Turner, D. D.: Improved ground-based liquid water path retrievals using a combined infrared and microwave approach, J. Geophys. Res. Atmospheres, 112(D15), D15204, doi:10.1029/2007JD008530, 2007.

Van Tricht, K., Lhermitte, S., Lenaerts, J. T. M., Gorodetskaya, I. V., L'Ecuyer, T. S., Noël, B., van den Broeke, M. R., Turner, D. D. and van Lipzig, N. P. M.: Clouds enhance Greenland ice sheet meltwater runoff, Nat. Commun., 7, 10266, doi:10.1038/ncomms10266, 2016.

Vaughan, M. A., Powell, K. A., Winker, D. M., Hostetler, C. A., Kuehn, R. E., Hunt, W. H., Getzewich, B. J., Young, S. A., Liu, Z. and McGill, M. J.: Fully Automated Detection of Cloud and Aerosol Layers in the CALIPSO Lidar Measurements, J. Atmospheric Ocean. Technol., 26(10), 2034–2050, doi:10.1175/2009JTECHA1228.1, 2009.

Wang, Z.: B-CLDCLASS-LIDAR Interface Control Document, [online] Available from: http://cswww.cira.colostate.edu/icd_pdf.php?avid=36&pvids=12 (Accessed 11 August 2016), 2013.

Wilcox, L. J., Highwood, E. J., Booth, B. B. B. and Carslaw, K. S.: Quantifying sources of inter-model diversity in the cloud albedo effect, Geophys. Res. Lett., 42(5), 2015GL063301, doi:10.1002/2015GL063301, 2015.

Winker, D. M., Vaughan, M. A., Omar, A., Hu, Y., Powell, K. A., Liu, Z., Hunt, W. H. and Young, S. A.: Overview of the CALIPSO Mission and CALIOP Data Processing Algorithms, J. Atmospheric Ocean. Technol., 26(11), 2310–2323, doi:10.1175/2009JTECHA1281.1, 2009.

Winker, D. M., Tackett, J. L., Getzewich, B. J., Liu, Z., Vaughan, M. A. and Rogers, R. R.: The global 3-D distribution of tropospheric aerosols as characterized by CALIOP, Atmos Chem Phys, 13(6), 3345–3361, doi:10.5194/acp-13-3345-2013, 2013.

Zamora, L. M., Kahn, R. A., Cubison, M. J., Diskin, G. S., Jimenez, J. L., Kondo, Y., McFarquhar, G. M., Nenes, A., Thornhill, K. L., Wisthaler, A., Zelenyuk, A. and Ziemba, L. D.: Aircraft-measured indirect cloud effects from biomass burning smoke in the Arctic and subarctic, Atmos Chem Phys, 16(2), 715–738, doi:10.5194/acp-16-715-2016, 2016.

Zhang, D., Wang, Z. and Liu, D.: A global view of midlevel liquid-layer topped stratiform cloud distribution and phase partition from CALIPSO and CloudSat measurements, , 115, D00H13, doi:10.1029/2009JD012143, 2010.

Zhang, Y., Seidel, D. J., Golaz, J.-C., Deser, C. and Tomas, R. A.: Climatological Characteristics of Arctic and Antarctic Surface-Based Inversions, J. Clim., 24(19), 5167–5186, doi:10.1175/2011JCLI4004.1, 2011.

Zhao, C. and Garrett, T. J.: Effects of Arctic haze on surface cloud radiative forcing, Geophys. Res. Lett., 2014GL062015, doi:10.1002/2014GL062015, 2015.

Atmos. Chem. Phys. Discuss., doi:10.5194/acp-2016-1037, 2016
Manuscript under review for journal Atmos. Chem. Phys.
Published: 14 December 2016

Atmospheric Chemistry and Physics Discussions

Table 1: Criteria used for cloud and air mass classification.

Data source type	Clean background clouds	All clouds	Aerosol-influenced clouds	Clear air
CALIPSO v. 3.01 L2 532 nm aerosol profile data				
Latitude: 60-82°N	x	x	x	x
Nighttime	x	x	x	x
Uppermost cloud layer only	x	x	x	
Surface elevation ≤ 4 km	x	x	x	
Cloud top altitude < 8 km asl	x	x	x	
Cloud base altitude > 1 km agl	x	x	x	
τ < ~3 (no extinction QC flag)	x	x	x	
In-cloud CAD score between 70-100	x	x	x	
CALIPSO "liquid"-phase only	x	x	x	
No cloud phase quality control flags	x	x	x	
No aerosol above cloud	x			
Aerosol observed above or below cloud			x	
No aerosol between cloud base and surface or next cloud top, whichever comes first	x			
Aerosol CAD score between -100 and -70			x	
No clouds or aerosol anywhere in profile				x
FLEXPART model output				
BC ≤ 30 ng C m^{-3}	x			
BC ≥ 30 ng C m^{-3}			x	
CloudSat 2B-CLDCLASS-LIDAR data				
Cloud top heights within 0.4 km of CALIPSO	x	x	x	
Liquid- or mixed-phase only	x	x	x	
Liquid-phase only (for r_{el} measurements)	x	x	x	

5

Atmos. Chem. Phys. Discuss., doi:10.5194/acp-2016-1037, 2016
Manuscript under review for journal Atmos. Chem. Phys.
Published: 14 December 2016

Atmospheric Chemistry and Physics Discussions

Table 2: Median (interquartile range) of Arctic marine cloud properties as classified by the criteria in Table 1, separated by reflectivity above and below detection limit (DL, -29 dBZ) and surface regime. Red (grey) color indicates significant (not significant) differences compared to clean background clouds, as determined at 95% confidence using a permutation test. Blue indicates that significance was lost[c] with altitude binning (relevant only to the open ocean cases). An asterisk indicates that the trend observed without binning was observed among all altitude bins, even though significance was not obtained (see Supplementary Table 1 for more details).

		Sea ice						Open ocean					
Attribute	**Z_m**	**Clean background**	**n**	**All clouds**	**n**	**Aerosol-impacted[a]**	**n**	**Background**	**n**	**All**	**n**	**Aerosol-impacted[a]**	**n**
Base T (°C)	> DL	-19.4 (-22.2 to -17.0)	1387	-19.9 (-22.6 to -17.4)	45 79	-20.1 (-23.5 to -17.7)	204	-16.6 (-19.7 to -10.4)	370	-14.4 (-19.1 to -9.4)	1734	-14.1 (-19.4 to -8.8)	125
	< DL	-21.5 (-24.6 to -18.2)	205	-19.8 (-23.0 to -16.6)	10 23	-18.7 (-22.8 to -16.0)	102	-14.7 (-19.5 to -7.6)	184	-10.2 (-17.9 to -4.7)	1049	-13.0 (-17.0 to -3.7)	89
	All	-19.6 (-22.5 to -17.2)	1604	-19.9 (-22.7 to -17.3)	56 91	-19.8 (-23.3 to -17.1)	314	-16.1 (-19.7 to -9.6)	571	-13.4 (-18.5 to -7.5) *	2919	-13.2 (-17.9 to -7.0)	223
Top T (°C)	> DL	-26.1 (-29.0 to -22.9)	1387	-25.9 (-28.6 to -22.4)	45 79	-25.3 (-28.9 to -21.8)	204	-24.4 (-28.2 to -19.0)	370	-21.1 (-26.5 to -15.3) *	1734	-19.8 (-25.6 to -14.3)	125
	< DL	-25.1 (-29.1 to -21.8)	205	-23.1 (-26.7 to -19.8)	10 23	-22.1 (-25.5 to -18.9)	102	-18.5 (-24.0 to -10.2)	184	-14.5 (-22.0 to -8.0)	1049	-15.9 (-21.1 to -7.6)	89
	All	-26.0 (-29.0 to -22.8)	1604	-25.4 (-28.4 to -21.9)	56 91	-24.2 (-28.4 to -20.2)	314	-22.5 (-27.1 to -15.5)	571	-19.1 (-24.9 to -11.8) *	2919	-18.0 (-23.5 to -11.5) *	223
Altitude, base (km)	> DL	1.8 (1.6-2.3)	1387	1.8 (1.5-2.3)	45 79	1.8 (1.5-2.5)	204	3.3 (2.4-4.0)	370	2.7 (1.8-3.6)	1734	2.4 (1.7-3.4) *	125
	< DL	2.5 (1.9-3.3)	205	2.1 (1.6-2.7)	10 23	2.2 (1.7-2.9)	102	3.3 (2.1-4.2)	184	2.5 (1.8-3.6)	1049	2.5 (1.7-3.0) *	89
	All	1.9 (1.6-2.5)	1604	1.8 (1.5-2.4)	56 91	2.0 (1.5-2.6)	314	3.3 (2.3-4.1)	571	2.6 (1.8-3.6)	2919	2.4 (1.7-3.3) *	223
Thickness (km)	> DL	1.2 (1.0-1.4)	1387	1.1 (0.7-1.3)	45 79	0.8 (0.6-1.0)	204	1.1 (0.7-1.6)	370	0.8 (0.7-1.4) *	1734	0.7 (0.7-1.1) *	125
	< DL	0.6 (0.5-0.7)	205	0.6 (0.5-0.7)	10 23	0.5 (0.5-0.7)	102	0.6 (0.4-0.7)	184	0.6 (0.5-0.7)	1049	0.6 (0.5-0.7)	89
	All	1.2 (0.8-1.4)	1604	0.9 (0.6-1.3)	56 91	0.7 (0.5-0.9)	314	0.8 (0.6-1.3)	571	0.7 (0.5-1.1)	2919	0.7 (0.5-0.9)	223
COD	> DL	1.2 (0.7-1.7)	937	1.1 (0.7-1.7)	33 70	0.8 (0.5-1.4)	175	0.9 (0.5-1.5)	301	1.0 (0.5-1.6)	1415	0.7 (0.4-1.2)	104
	< DL	0.4 (0.3-0.7)	184	0.6 (0.3-1.0)	88 0	0.5 (0.3-0.8)	77	0.3 (0.2-0.6)	163	0.5 (0.2-1.1)	847	0.6 (0.3-1.4)	73
	All	1.0 (0.5-1.7)	1132	1.0 (0.5-1.6)	43 31	0.7 (0.4-1.2)	259	0.7 (0.3-1.2)	479	0.8 (0.3-1.5)	2362	0.7 (0.4-1.2)	185

Atmos. Chem. Phys. Discuss., doi:10.5194/acp-2016-1037, 2016
Manuscript under review for journal Atmos. Chem. Phys.
Published: 14 December 2016

Atmospheric Chemistry and Physics Discussions

Multi-layer clouds	> DL	39%	1387	41%	4579	69%	204	75%	370	71%	1734	83%	125
	< DL	60%	205	56%	1023	86%	102	92%	184	80% *	1049	90%	89
	All	42%	1604	44%	5691	75%	314	81%	571	75% *	2919	86%	223
BC at base (ng m^{-3})	> DL	15 (11-22)	1387	27 (14-56)	4579	56 (42-82)	204	15 (11-21)	370	20 (11-38)	1734	62 (40-94)	125
	< DL	15 (12-20)	205	22 (13-43)	1023	45 (38-80)	102	13 (8-19)	184	19 (10-38)	1049	57 (40-94)	89
	All	15 (11-22)	1604	26 (14-51)	5691	54 (39-81)	314	14 (10-20)	571	19 (11-38)	2919	61 (40-94)	223
% Mixed-phase	> DL	100%	63	97%	146	100%	8	93%	138	88%	412	72%	18
% precipitating[b]	> DL	20%	1571	14%	4811	8%	196	10%	383	8%	1675	4%	114
r_e (μm)	> DL	10.5 (9.7-11.4)	1178	10.3 (9.5-11.3)	3809	10.0 (9.4-11.1)	152	10.2 (9.4-11.2)	284	10.3 (9.4-11.4)	1211	10.0 (9.0-11.0)	78
Reflectivity (dBZ)	> DL	-19.6 (-23.6 to -17.3)	1349	-20.8 (-24.5 to -16.9)	4462	-22.2 (-25.6 to -18.8)	197	-21.8 (-25.8 to -17.3)	368	-21.4 (-25.9 to -16.6)	1729	-23.4 (-26.8 to -16.9)	204

[a]**Aerosol-impacted, as determined in the third column of Table 1.**

[b]**Precipitating clouds were included in this metric only; for all other attribute classifications, clouds were required to have no observed precipitation.**

[c]**Significance was presumed to be lost across altitude bins when there were multiple cases of non-significance among altitude bins or different trends in significance between altitude bins.**

Atmos. Chem. Phys. Discuss., doi:10.5194/acp-2016-1037, 2016
Manuscript under review for journal Atmos. Chem. Phys.
Published: 14 December 2016

Atmospheric Chemistry and Physics Discussions

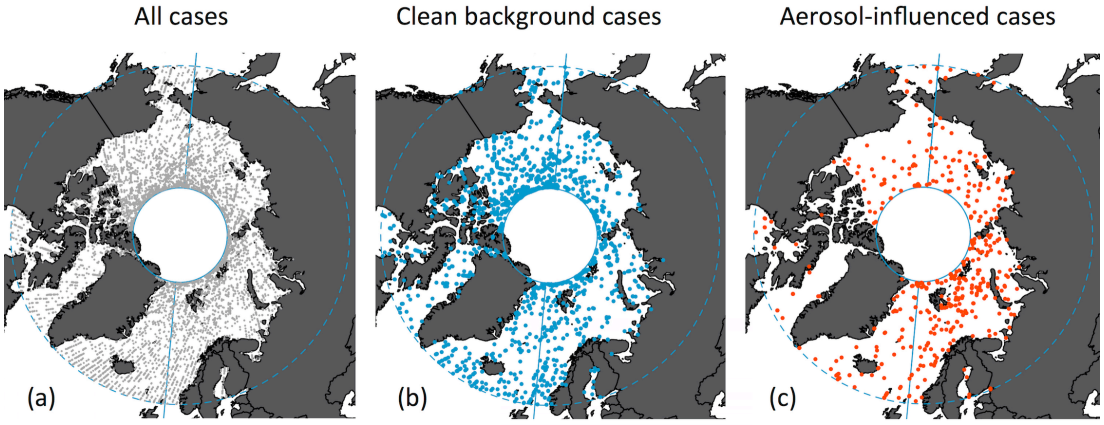

Figure 1: The geographical distribution of cloud profiles, where (a) grey indicates all cases, (b) blue indicates clean background cases, and (c) red indicates aerosol-influenced cases.

5

Atmos. Chem. Phys. Discuss., doi:10.5194/acp-2016-1037, 2016
Manuscript under review for journal Atmos. Chem. Phys.
Published: 14 December 2016

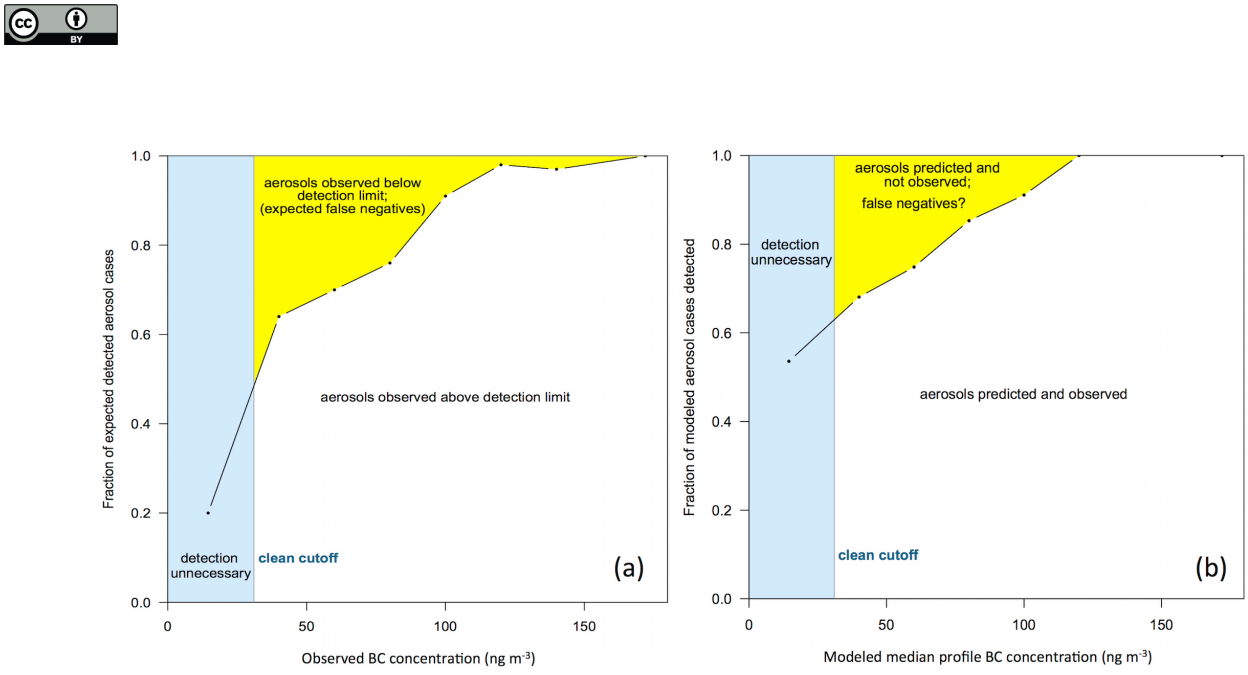

Figure 2: Based on CALIPSO Arctic profiles under non-cloudy conditions, we compare a) the expected fraction and b) possible maximum fraction of false negatives (aerosol present but not detected) for different aerosol concentrations and/or combustion tracers. Tracers include black carbon (BC, ng C m^{-3}) and the concentration of aerosols with diameters > 0.12 µm (CN_{PCASP}, cm^{-3}). The expected fraction of false negatives in panel a) was determined by comparing binned out-of-cloud 2008 ARCTAS-A and -B BC concentrations and ISDAC CN_{PCASP} concentrations with the fraction of the total number of samples between 1-5 km that had converted backscatter values (Mm^{-1} sr^{-1}) above the CALIPSO clear-sky nighttime backscatter detection limit from Winker et al. (2009) (see text for more details). Possible maximum false negative values in panel b) were determined by comparing the FLEXPART model's median BC concentrations between 0-10 km with the fraction of the total CALIPSO profiles under non-cloudy conditions during January, 2008 where aerosols were not detected. The clean cutoff below which air is taken as "clean" is assumed to be 31 ng C m^{-3} and 127 cm^{-3} for BC and CN_{PCASP}, respectively.

Atmos. Chem. Phys. Discuss., doi:10.5194/acp-2016-1037, 2016
Manuscript under review for journal Atmos. Chem. Phys.
Published: 14 December 2016

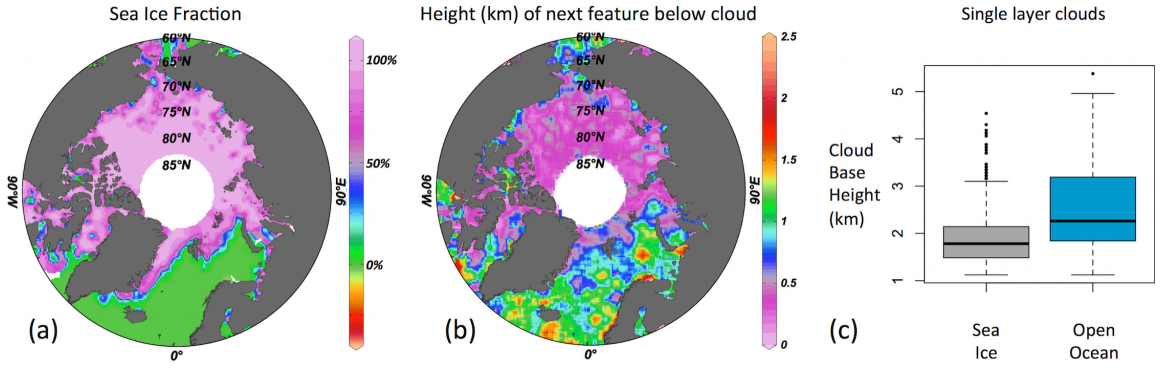

Figure 3: The data shown in a) and b) are weighted-average gridded maps of features below individual cloud points for a) sea ice fraction, and b) height of the next lowest feature associated with individual cloud profiles, where a value of 0 indicates that the ocean surface was the next lowest feature. Over open ocean, multi-layer clouds were much more common than over sea ice. Shown in c) is a boxplot indicating the cloud base heights (km) for single layer clouds over sea ice (grey) and open ocean (blue).

Atmos. Chem. Phys. Discuss., doi:10.5194/acp-2016-1037, 2016
Manuscript under review for journal Atmos. Chem. Phys.
Published: 14 December 2016

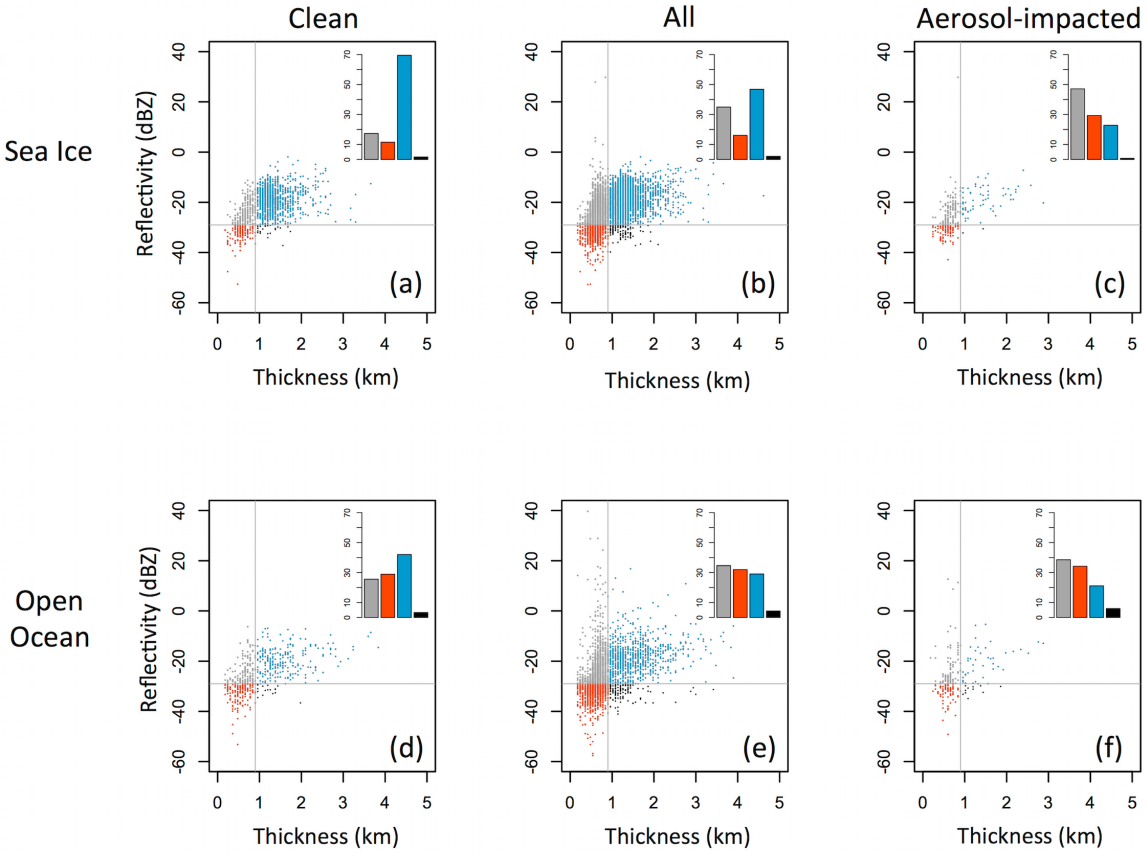

Figure 4: A comparison of CALIPSO cloud thickness (km) with CloudSat reflectivity (dBZ), as separated by sea ice and open ocean regimes, and by clouds found in conditions labeled as clean background, all conditions, and aerosol-impacted conditions. To better show changes in the two parameters, plots have been divided into four quadrants (above (grey and blue) and below (orange and black) the CloudSat reflectivity detection limit of -29 dBZ), and above (blue and black) and below (orange and grey) a thickness of 0.9 km. In the supper right of each plot is shown the fraction of cases within each quadrant, following the quadrant color scheme.